

## Load current balancing for 4-wire systems using harmonic treated TCR based SVCs

Abdulkareem Mokif Obais<sup>1</sup>, Ali Abdulkareem Mukheef<sup>2</sup>

<sup>1</sup>Department of Biomedical Engineering, College of Engineering, University of Babylon, Babylon, Iraq

<sup>2</sup>English Department, Almustaqbal University College, Babylon, Iraq

### Article Info

#### Article history:

Received Jun 25, 2022

Revised Jun 30, 2022

Accepted Jul 6, 2022

#### Keywords:

Energy saving

Harmonic cancellation

Load compensation

Power quality

Reactive power control

### ABSTRACT

In this paper, a harmonic-treated thyristor-controlled reactor TCR is presented as a linearized harmonic-free compensating susceptance controllable in inductive and capacitive modes. The harmonic-treated TCR is a traditional TCR conditioned in such a manner that it can respond continuously and linearly to capacitive and inductive reactive current demands without noticeable harmonic association or active power contribution. The conditioned configuration is produced by equipping the TCR with self-harmonic suppressing and filtering circuitries, which guarantee harmonic cancellation with minimal no load operating losses. The harmonic treated TCR avoids the need to high power harmonic filters required to treat the harmonics of the traditional TCR. The devised susceptances are used to build a load current balancing system for grounded loads in a 380-V, 50Hz power distribution system. Both the compensating susceptances and the load current balancing system were designed and tested on PSpice. The simulation results have demonstrated the linearity, control continuity, and harmonic cancellation of the proposed harmonic-treated TCR as a fast response compensating susceptance reliable for load current balancing purposes. The proposed load current balancing system revealed superior treatment to various unbalance conditions, thus it is deservedly promoted to have the feasibility of supporting grids having fast varying loads.

This is an open access article under the [CC BY-SA](https://creativecommons.org/licenses/by-sa/4.0/) license.



### Corresponding Author:

Abdulkareem Mokif Obais

Department of Biomedical Engineering, College of Engineering, University of Babylon

Al Najaf's Street, Al Hillah, Babylon, Iraq

Email: karimobais@yahoo.com

## 1. INTRODUCTION

Unbalanced loads and loads with poor power factor are two challenging issues facing the power quality of power system networks. Reactive power (Var) is mainly controlled by static Var compensators. Var control is usually employed to meet power quality requirements such as voltage regulation and power factor correction. Many power quality issues such as harmonic minimization and load compensation can be solved by using static Var compensators or static compensators [1]-[7]. The difference between a static Var compensator (SVC) and static compensator is that a static Var compensator is a reactive device used to control Var in both modes of operations (inductive and capacitive), while a static compensator is capable of controlling both real power and reactive power. A static compensator may be constructed of several SVCs. The increase in electricity demand nowadays makes focusing on power quality greater than ever. Today, there is an urgent need to increase the efficiency of transmission systems by minimizing their losses through load compensation and power factor correction [8], [9]. Static Var compensators and static compensators are

efficient tools to accomplish load compensation and power factor correction for better power quality purposes [10]. The thyristor-controlled reactor TCR is simply a reactor connected in series to two anti-parallel thyristors and the series combination is supplied by a phase or line to line voltage of the AC power system network. It is controlled continuously by the symmetrical firing angles of its thyristors. TCR usually injects odd harmonic current components [1], thus it requires installation of harmonic filters at its location [5]. Poor power factor and unbalanced loads cause extra losses in transmission systems and power generation stations. In addition, they may restrict the transmission capability of transmission systems. Therefore, load compensation and power factor correction are effective remedies to these challenging issues. The benefits of load compensation and power factor correction are involved in energy saving, transmission loss reduction, voltage stabilization, and the feasibility of operating transmission lines closer to their thermal limits [11]-[25].

Load compensation and power factor correction systems have great impacts in transmission loss reduction and energy saving in power generation stations [11]-[25]. Load currents balancing process is involved in two steps; load reactive currents compensation which means power factor correction and load active power compensation which means load balancing [8]-[11]. Load compensation and power factor correction were firstly approached by using static Var compensators in 1978 by [25]. At that time the TCR was available as controllable inductive reactive device. It was used beside a fixed capacitor to devise a static Var compensator controllable in inductive and capacitive modes of operation. Three identical fixed capacitor-thyristor controlled reactor based switched virtual circuit SVCs were connected in delta-form and used to compensate load unbalances for ungrounded loads. In this work load balancing mechanism was studied and its compensating susceptances basic equations were derived in terms of load conductances and susceptances using symmetrical components. The compensation system was designed for load balancing of three-wire unbalanced loads. The compensation process comprised two steps; unity power correction and real power balancing. Although the compensation system released a wide spectrum of odd current harmonics, it opened wide spaces of interest in load compensation by using static Var compensators. Actually, static Var compensators employing TCRs in their construction require high power harmonic filters which add additional costs and energy losses [1]. Large fluctuating loads are intended to be balanced for two main reasons: 1- the AC power system is too weak to support its terminal voltage within acceptable range of variation and 2- it is not economical or practical to supply Var demand from the AC system [23]. Load current balancing systems require pure compensating susceptances in order to compensate the load reactive current components and balance its active current components. Load current balancing for 4-wire systems can be achieved using power converter based Var devices like distribution static synchronous compensators STATCOMs distribution static synchronous compensator (DSTATCOM) [2], [8], [25]. Other approaches adopted shunt power converted based Var compensating devices for accomplishing voltage and current compensation in addition to harmonic minimization [2], [4], [6], [7], [12], [13], [20]. Series compensation systems can be used for treating voltage and current imbalance conditions beside the treatment of harmonic issues [15]. Separate compensating susceptances connected in delta and star forms are capable of accomplishing more flexible compensation for voltage and current imbalance conditions compared to systems using lumped compensation systems like DSTATCOMs [1], [3], [5], [8]-[11], [14]-[19], [21], [22].

Newton-Raphson method was used in [26] to model the TCR in frequency domain for accomplishing fast convergence to steady state with high accuracy. A cascaded single-phase converter having seven voltage levels was built by [27] using a hybrid of two-level cells. This scheme requires reduced number of switching devices compared traditional ones. It is designed to integrate two-stage cells for shaping the intended voltage profile. Similar topology was approached by [28] to reduce the harmonic effect on the converter voltage profile. A shunt active power filter was proposed by [29] for treating the problem harmonics current in the AC source as a result of nonlinear loads. This filter was designed to improve the power quality of the AC grid via compensating harmonic currents and reactive power. A single-phase voltage source converter equipped with a shunt active filter was proposed by [30] to accomplish optimal minimization of current disturbance and harmonic reduction. A DSTATCOM equipped with  $Icos\phi$  controlling modality was proposed by [30] to enhance voltage regulation, power factor improvement, load balancing, and harmonic suppression of non-linear loads, whereas a system in [31].

In this work, a new configuration of compensating susceptances characterized by control continuity, broad range of linearity, negligible no load operating losses, very low operating losses, considerable fast response to current demand, and negligible harmonic injection. The proposed susceptances are built of harmonic-treated TCRs and employed in the construction of two static compensators for balancing phase currents in 4-wire systems. Applying the new proposed compensating devices in the construction of the proposed load balancing system, results in wide range of compensation capability, high speed response in fast varying environments, perfect balancing of AC source line currents, and stiff synchronization with utility grid.

## 2. LOAD CURRENT BALANCING FOR THREE-PHASE, 4-WIRE LOADS

For an unbalanced grounded wye-connected load, a current flow through the neutral wire. Therefore, load current balancing for three-phase, 4-wire loads requires two static compensators in order to achieve active phase currents balancing and reactive currents compensation [9], [14]. The first static compensator is connected in delta-form using three identical compensating susceptances controlled continuously in capacitive and inductive modes of operation. The second static compensator is similar to first one except its compensating susceptances are connected in star-form. Figure 1 shows the layout of the balancing mechanism of a three-phase, 4-wire load (grounded load) fed by a balanced three phase voltages  $V_A$ ,  $V_B$ , and  $V_C$ . The mechanism of this technique is involved in two steps. In the first step, the active current components of the load phase currents are balanced by the active current components of the line currents produced by the delta-connected static compensator. In the second step, the reactive current components produced by the delta-connected static compensator and the reactive current components of the load phase currents are compensated by the reactive phase currents produced by the star-connected static compensator.  $B_{S1AB}$ ,  $B_{S1BC}$ , and  $B_{S1CA}$  are the compensating susceptances of the first compensator (delta-connected static compensator), while  $B_{S2A}$ ,  $B_{S2B}$ , and  $B_{S2C}$  are compensating susceptances of the second static compensator (star-connected static compensator).  $I_{S1A}$ ,  $I_{S1B}$ , and  $I_{S1C}$  are the first static compensator line currents, while  $I_{S2A}$ ,  $I_{S2B}$ , and  $I_{S2C}$  are the phase currents of the second static compensator.  $I_{LA}$ ,  $I_{LB}$ , and  $I_{LC}$  are load phase or line currents.

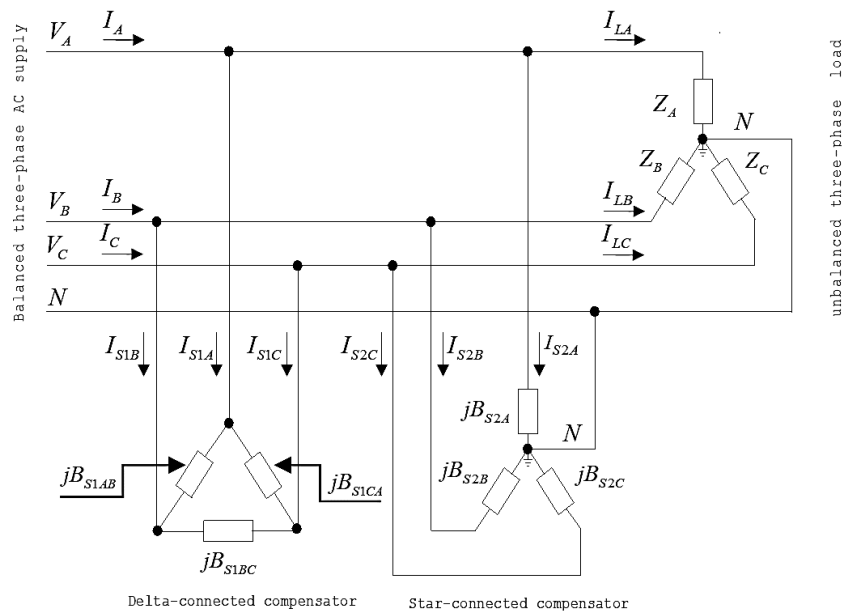


Figure 1. Layout of load current balancing system for grounded loads

The AC phase voltages  $V_A$ ,  $V_B$ , and  $V_C$  of the three-phase power system network are assumed to be balanced, thus they can be given by:

$$V_A = V \quad (1)$$

$$V_B = V \angle \left(-\frac{2\pi}{3}\right) \quad (2)$$

$$V_C = V \angle \left(-\frac{4\pi}{3}\right) \quad (3)$$

Where,  $V$  is the rms magnitude of each phase voltage and  $\angle$  represents the phase angle symbol. The phase currents of the unbalanced three-phase 4-wire load can be given by

$$I_{LA} = |I_{LA}| \angle \phi_{LA} = |I_{LA}| \cos \phi_{LA} + j |I_{LA}| \sin \phi_{LA} \quad (4)$$

$$I_{LB} = |I_{LB}| \angle \left( -\frac{2\pi}{3} + \phi_{LB} \right) = (|I_{LB}| \cos \phi_{LB} + j|I_{LB}| \sin \phi_{LB}) \angle \left( -\frac{2\pi}{3} \right) \quad (5)$$

$$I_{LC} = |I_{LC}| \angle \left( -\frac{4\pi}{3} + \phi_{LB} \right) = (|I_{LC}| \cos \phi_{LC} + j|I_{LC}| \sin \phi_{LC}) \angle \left( -\frac{4\pi}{3} \right) \quad (6)$$

Where,  $\phi_{LA}$ ,  $\phi_{LB}$ , and  $\phi_{LC}$  are the power factor angles of phases A, B, and C respectively.  $|I_{LA}|$ ,  $|I_{LB}|$ , and  $|I_{LC}|$ , are the absolute rms values of  $I_{LA}$ ,  $I_{LB}$ , and  $I_{LC}$  respectively.  $I_A$ ,  $I_B$ , and  $I_C$  are the rms line currents of the AC source. According to the main objective of this research, the AC source currents should be balanced and active. Consequently, they can be expressed as:

$$I_A = I \quad (7)$$

$$I_B = I \angle \left( -\frac{2\pi}{3} \right) \quad (8)$$

$$I_C = I \angle \left( -\frac{4\pi}{3} \right) \quad (9)$$

Where,  $I$  is the rms magnitude of each phase current. The active power  $P_L$  supplied to the unbalanced load and the active power  $P$  that should be supplied by the AC source after balancing can be given by:

$$P_L = V(|I_{LA}| \cos \phi_{LA} + |I_{LB}| \cos \phi_{LB} + |I_{LC}| \cos \phi_{LC}) \quad (10)$$

$$P = 3VI \quad (11)$$

The active power supplied by the AC source should be equal to the power consumed by the unbalanced load or in other words:

$$P = 3VI = P_L = V(|I_{LA}| \cos \phi_{LA} + |I_{LB}| \cos \phi_{LB} + |I_{LC}| \cos \phi_{LC}) \quad (12)$$

In (12) for  $I$ , gives

$$I = \frac{|I_{LA}| \cos \phi_{LA} + |I_{LB}| \cos \phi_{LB} + |I_{LC}| \cos \phi_{LC}}{3} \quad (13)$$

The compensating currents  $I_{S1A}$ ,  $I_{S1B}$ , and  $I_{S1C}$  of the delta-connected static compensator can be expressed in terms of its compensating susceptances and phase voltages as:

$$I_{S1A} = \sqrt{3}V \cos \left( \frac{\pi}{3} \right) (B_{S1CA} - B_{S1AB}) + j\sqrt{3}V \sin \left( \frac{\pi}{3} \right) (B_{S1AB} + B_{S1CA}) \quad (14)$$

$$I_{S1B} = \left( \sqrt{3}V \cos \left( \frac{\pi}{3} \right) (B_{S1AB} - B_{S1BC}) + j\sqrt{3}V \sin \left( \frac{\pi}{3} \right) (B_{S1BC} + B_{S1AB}) \right) \angle \left( -\frac{2\pi}{3} \right) \quad (15)$$

$$I_{S1C} = \left( \sqrt{3}V \cos \left( \frac{\pi}{3} \right) (B_{S1BC} - B_{S1CA}) + j\sqrt{3}V \sin \left( \frac{\pi}{3} \right) (B_{S1CA} + B_{S1BC}) \right) \angle \left( -\frac{4\pi}{3} \right) \quad (16)$$

According to [9], [14], the compensating susceptances  $B_{S1AB}$ ,  $B_{S1BC}$ , and  $B_{S1CA}$  can be expressed in terms of load active current components as:

$$B_{S1AB} = \frac{2}{3\sqrt{3}V} (|I_{LA}| \cos \phi_{LA} - |I_{LB}| \cos \phi_{LB}) \quad (17)$$

$$B_{S1BC} = \frac{2}{3\sqrt{3}V} (|I_{LB}| \cos \phi_{LB} - |I_{LC}| \cos \phi_{LC}) \quad (18)$$

$$B_{S1CA} = \frac{2}{3\sqrt{3}V} (|I_{LC}| \cos \phi_{LC} - |I_{LA}| \cos \phi_{LA}) \quad (19)$$

Both the delta-connected static compensator (the first static compensator) and the Y-connected compensator (the second static compensator) are built of pure susceptances and don't consume any active power at all. The susceptance currents  $I_{S2A}$ ,  $I_{S2B}$ , and  $I_{S2C}$  of the second compensator are pure reactive and should compensate for the reactive currents generated by the first compensator and the load reactive currents. Doing this for each phase of the second compensator and substituting for  $B_{S1AB}$ ,  $B_{S1BC}$ , and  $B_{S1CA}$  by its values expressed in (17)-

(19) give positive values of compensating susceptances denote capacitive susceptances, while negative values mean inductive susceptances.

$$B_{S2A} = \frac{|I_{LB}| \cos \phi_{LB} - |I_{LC}| \cos \phi_{LC} - \sqrt{3} |I_{LA}| \sin \phi_{LA}}{\sqrt{3}V} \quad (20)$$

$$B_{S2B} = \frac{|I_{LC}| \cos \phi_{LC} - |I_{LA}| \cos \phi_{LA} - \sqrt{3} |I_{LB}| \sin \phi_{LB}}{\sqrt{3}V} \quad (21)$$

$$B_{S2C} = \frac{|I_{LA}| \cos \phi_{LA} - |I_{LB}| \cos \phi_{LB} - \sqrt{3} |I_{LC}| \sin \phi_{LC}}{\sqrt{3}V} \quad (22)$$

## 2.1. The harmonic-treated TCR based SVC

The harmonic-treated TCR is built of a harmonic-suppressing circuit connected in series with a traditional TCR shunted by a filtering circuit as shown in Figure 2. The filtering circuit is responsible for the cancellation of the harmonics released by the TCR and generating the capacitive reactive power demanded from the SVC. The harmonic-treated TCR is a reliable replacement of the traditional fixed-capacitor thyristor controlled-reactor shunted by high power harmonic filters. In addition, the harmonic-treated TCR current fundamental is linearized with reactive current demand.

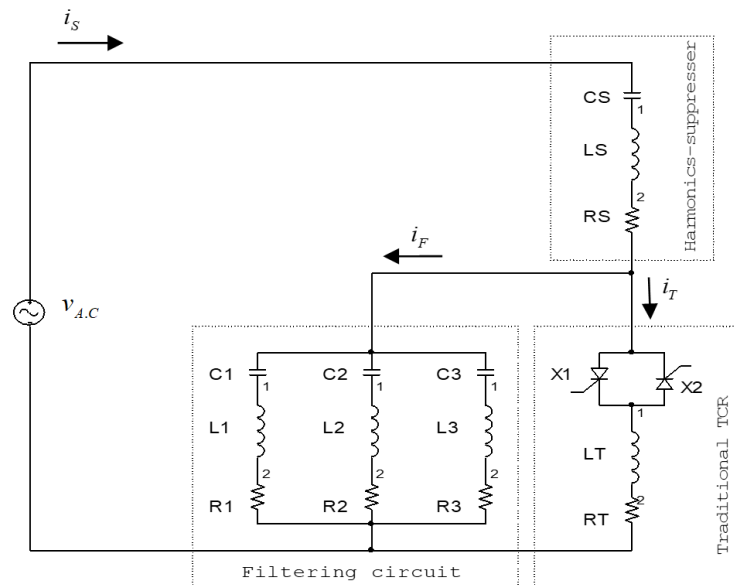


Figure 2. Layout of the harmonic-treated TCR based SVC

The harmonic-suppressing circuit is built of the series RLC circuit represented by  $C_S$ ,  $L_S$ , and  $R_S$ . It is designed to resonate at the AC source fundamental angular frequency  $\omega$ .  $R_S$  represents the self-resistance of the reactor  $L_S$ . The filtering circuit is built of the series RLC filters  $R_1L_1C_1$ ,  $R_2L_2C_2$ , and  $R_3L_3C_3$  which are designed to eliminate, respectively the third, fifth, and seventh odd current harmonics released by the TCR.  $R_1$ ,  $R_2$ , and  $R_3$  are the self-resistances of  $L_1$ ,  $L_2$ , and  $L_3$ , respectively. The currents  $i_S$ ,  $i_T$ , and  $i_F$  are representing the instantaneous currents of the SVC, TCR, and the filtering circuit, respectively. The traditional TCR and its current waveform are shown in Figure 3. In this figure, the TCR is represented by the reactor  $L_T$  and the two anti-parallel thyristors  $X_1$  and  $X_2$ . The AC instantaneous voltage applied across the TCR is  $v_T$ , while  $\alpha$  represents its firing angle which is measured from positive peak point of  $v_T$  toward its next negative slope zero-crossing point. This angle varies in the range of  $0 \leq \alpha \leq \pi/2$ . The fundamental component of  $i_T$  can be given by [1], [5], [26].

$$I_1 = \frac{V_m}{\pi \omega L_T} (\pi - 2\alpha - \sin 2\alpha) = \frac{V_m}{\omega L_T} F(\alpha) \quad (23)$$

Where  $F(\alpha)$  is defined by:

$$F(\alpha) = \left(1 - \frac{2\alpha}{\pi} - \frac{\sin 2\alpha}{\pi}\right) \quad (24)$$

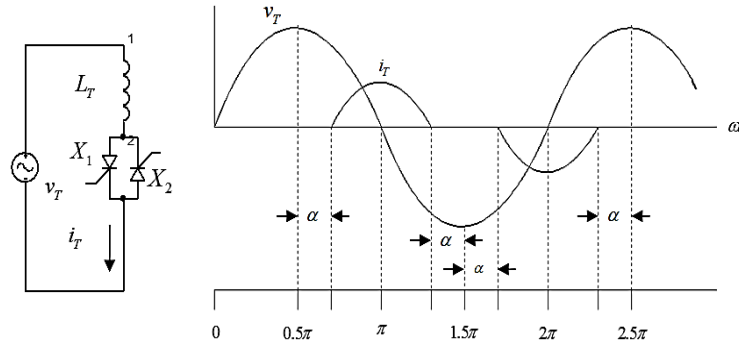


Figure 3. The traditional TCR and its actual current waveforms

The instantaneous value of fundamental component of  $i_T$  is  $i_1$ , which can be expressed as in (25):

$$i_1 = -I_1 \cos(\omega t) = -\frac{V_m}{\omega L_T} F(\alpha) \cos(\omega t) \quad (25)$$

Since  $i_T$  is symmetrical around the  $\omega t$  axis, it only contains odd harmonic current components. The absolute value of its  $n$ th current harmonic is given by [1], [5].

$$I_n = \frac{4V_m}{\pi\omega L_T} \left( \frac{\sin \alpha \cos(n\alpha) - n \cos \alpha \sin(n\alpha)}{n(n^2-1)} \right) \quad (26)$$

Where,  $n$  is a non-unity positive odd integer. Since the harmonic-suppressing circuit is designed such that it resonates at the AC fundamental frequency  $\omega$ , it can be written.

$$X_S = \omega L_S = \frac{1}{\omega C_S} \quad (27)$$

Where,  $X_S$  is the characteristic impedance of the harmonic-suppressing circuit. Since the harmonic filters  $R_1L_1C_1$ ,  $R_2L_2C_2$ , and  $R_3L_3C_3$  resonate at  $3\omega$ ,  $5\omega$ , and  $7\omega$ , respectively, the following can be deduced.

$$X_3 = 3\omega L_1 = \frac{1}{3\omega C_1} \quad (28)$$

$$X_5 = 5\omega L_2 = \frac{1}{5\omega C_2} \quad (29)$$

$$X_7 = 7\omega L_3 = \frac{1}{7\omega C_3} \quad (30)$$

Where,  $X_3$ ,  $X_5$ , and  $X_7$  are the characteristic impedances of the harmonic filters  $R_1L_1C_1$ ,  $R_2L_2C_2$ , and  $R_3L_3C_3$ , respectively. At frequencies of order higher than that of the 7<sup>th</sup> harmonic, the self-resistances of the reactors building the filtering and the harmonic-suppressing circuits become negligible compared to their corresponding reactances. Consequently, the  $n$ th harmonic impedances of the filtering circuit  $Z_F(n\omega)$  and harmonic-suppressing circuit  $Z_S(n\omega)$  can be expressed as:

$$Z_F(n\omega) = \frac{j}{\frac{1}{n\omega L_1 - \frac{1}{n\omega C_1}} + \frac{1}{n\omega L_2 - \frac{1}{n\omega C_2}} + \frac{1}{n\omega L_3 - \frac{1}{n\omega C_3}}}, n > 7 \quad (31)$$

$$Z_S(n\omega) = jn\omega L_S + \frac{1}{jn\omega C_S} = jX_S \frac{n^2-1}{n}, n > 7 \quad (32)$$

The  $n$ th harmonic impedance of the harmonic-suppressing circuit is required to be very much greater than that of the filtering circuit at frequencies above the 7<sup>th</sup> harmonic in order to protect AC grid from the injection of higher current harmonics. This implies that as in (33):

$$|Z_S(n\omega)| \geq 10|Z_F(n\omega)| \quad (33)$$

If the filtering circuit is designed such that its harmonic filters have the same characteristic impedances at their corresponding resonance frequencies, then  $Z_F(n\omega)$  can be simplified to:

$$Z_F(n\omega) = \frac{j}{\frac{1}{\frac{nZ_0}{3} + \frac{3Z_0}{n}} + \frac{1}{\frac{nZ_0}{5} + \frac{5Z_0}{n}} + \frac{1}{\frac{nZ_0}{7} + \frac{7Z_0}{n}}} = \frac{jZ_0}{\frac{3n}{n^2-9} + \frac{5n}{n^2-25} + \frac{7n}{n^2-49}}, n > 7 \quad (34)$$

Where  $Z_0$  is defined by:

$$Z_0 = X_3 = X_5 = X_7 \quad (35)$$

Substituting (32) and (34) into (33) gives:

$$X_S \geq \frac{10Z_0}{(n^2-1)\left(\frac{3}{n^2-9} + \frac{5}{n^2-25} + \frac{7}{n^2-49}\right)}, n > 7 \quad (36)$$

Changing the ( $\geq$ ) operation to ( $=$ ) in (36) and taking  $n=9$  yield:

$$X_S = \frac{84}{235}Z_0 \quad (37)$$

The harmonic filters in the SVC depicted in Figure 2 are responsible for supplying the capacitive reactive current demand. The maximum value of this current is supplied when the TCR firing angle is  $\pi/2$ . At zero reactive current demand, the TCR must be fired at an angle such that it compensates for the capacitive current generated by the filtering circuit. On the other hand, this SVC must be capable of satisfying its inductive reactive current demand. The reactive current ratings (capacitive and inductive) of the SVC employed in the star-connected compensator are mainly dependent on the reactive current rating of the SVC employed in the delta-connected compensator and the average power factor of the three-phase load intended to be balanced. Since the SVC employed in delta-connected compensator represents a bipolar compensating susceptance, it should have similar inductive and capacitive current ratings, i.e. the TCR reactive current rating should be twice that of the filtering circuit. Generally, taking the TCR and filtering circuit reactive current ratings into accounts, implies that:

$$|Z_F(\omega)| = k_R \omega L_T \quad (38)$$

Where,  $k_R$  is the rating factor which indicates how much the TCR reactive rating is greater than that of the filtering circuit. At the supply fundamental angular frequency  $\omega$ , the filtering circuit becomes to some extent pure capacitive. In other words, the harmonic filters self-resistances become negligible compared to their corresponding net capacitive reactances. Taking  $n=1$  in (34) and substituting for  $Z_F(\omega)$  in (38) give:

$$Z_0 = \frac{35}{48}k_R \omega L_T \quad (39)$$

Substituting (37) into (39) and equating for  $L_1$ ,  $L_2$ , and  $L_3$  in (28)-(30), respectively, give:

$$L_1 = \frac{35}{144}k_R L_T \quad (40)$$

$$L_2 = \frac{7}{48}k_R L_T \quad (41)$$

$$L_3 = \frac{5}{48}k_R L_T \quad (42)$$

Substituting (39) into (37) and equating for  $L_S$  in (27) give:

$$L_S = \frac{49}{188} k_R L_T \quad (43)$$

The capacitor's design values can be determined using the expressions identified in (27)-(30). The self-resistances of reactors are chosen such that their corresponding reactors are revealing almost pure reactive responses at the AC source fundamental frequency. The harmonic-suppressing and filtering circuits function coherently to block the flowing of TCR current harmonics in the AC source side. In addition, these circuitries achieve cost and energy savings compared with the high power harmonic filters required for the traditional TCR applications.

### 2.1.1. SVC current controlling scheme

The current controlling strategy of the SVC built of a harmonic-treated TCR is shown in Figure 4. The input signals in this figure are  $k_2 B_S$  and  $k_3 v_{AC}$ . The analogue signal  $k_2 B_S$  is actually proportional to the reactive current demanded from the SVC.  $V_{CT}$  is an analogue voltage controlling the TCR firing angle and is determined as:

$$V_{CT} = 5A_1 - A_2 k_2 B_S \quad (44)$$

Where,  $A_1$  and  $A_2$  are constants depending on the rating factor  $K_R$ .  $V_{CT}$  varies in the range of zero to +5V. The zero value corresponds to the maximum positive value of  $k_2 B_S$ , while +5V is corresponding to its lowest negative value. The voltage signal  $k_3 v_{AC}$  is firstly zero-crossed to produce the rectangular waveform  $V_{S1}$  and secondly delayed by 5msec and then zero-crossed to produce the rectangular waveform  $V_{S2}$ . The rectangular waveform  $V_{S3}$  is obtained through the X-NOR operation on  $V_{S1}$  and  $V_{S2}$ .  $V_{S3}$  is processed in  $F(\alpha)$  block which produces a waveform representing the analogue simulation of in (24). The output of  $F(\alpha)$  is multiplied by 5 to obtain  $V(\alpha)$ .  $V_{CT}$  is compared with  $V(\alpha)$  to obtain  $V_{CX}$  which is logically multiplied by  $V_{S2}$  and its complement to obtain the TCR firing signals  $V_{X1}$  and  $V_{X2}$  shown in Figure 5. The TCR firing signals can be given by:

$$V_{X1} = V_{CX} V_{S2} \quad (45)$$

$$V_{X2} = V_{CX} \overline{V_{S2}} \quad (46)$$

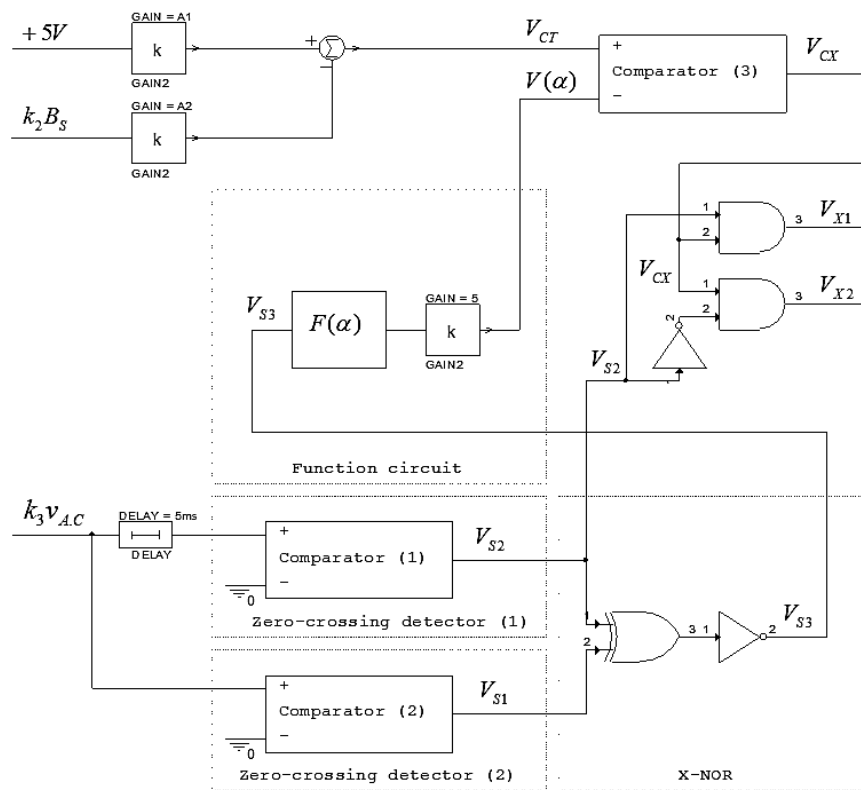


Figure 4. The harmonic-treated TCR controlling scheme



The static Var compensator absolute rms current rating  $|I_{SR}|$  can be given by (47):

$$|I_{SR}| = |B_S V_{AC}| \quad (47)$$

Where,  $V_{AC}$  is the rms voltage applied across the SVC and  $B_S$  is its compensating susceptance. For the harmonic-treated TCR,  $B_S$  represents the compensating susceptance constituted by the filtering circuit and the TCR circuit. The rms current of the harmonic-treated TCR based SVC can be expressed in terms of the filtering circuit parameters, TCR reactance, and  $V_{CT}$  as:

$$I_S = jB_S V_{AC} = -jV_{AC} \left( \frac{1}{\omega L_1 - \frac{1}{\omega C_1}} + \frac{1}{\omega L_2 - \frac{1}{\omega C_2}} + \frac{1}{\omega L_3 - \frac{1}{\omega C_3}} + \frac{0.2V_{CT}}{\omega L_T} \right) \quad (48)$$

When  $V_{CT}$  is zero, this SVC is supplying its maximum capacitive current, while it absorbs its maximum inductive current when  $V_{CT}$  is +5V.

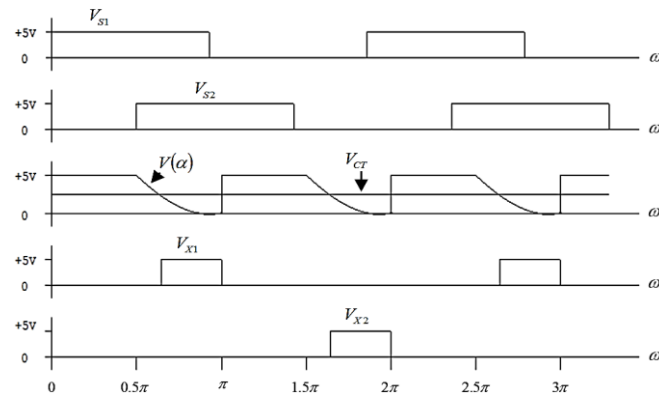


Figure 5. The TCR firing signals determination process

## 2.2. Circuit design of the 380-V, 50-Hz harmonic-treated TCR based SVC

The harmonic-treated TCR based SVC represents the building block of the load current balancing system of the three-phase unbalanced grounded load. This system is designed for load currents balancing of a 100-kVA, 11kV/ 380V power transformer in 380-V, 50-Hz Iraqi distribution network. The rated line (phase) current of this transformer at its secondary side (consumer side), is about 214A (peak value). The average power factor for its phase currents is considered to be about 0.8 lagging. The load current balancing system for grounded loads has two static compensators; the first is built of three identical SVCs of type SVC1 connected in delta-form, while the second compensator is built of three identical SVCs of type SVC2 connected in star-form. Actually, SVC1 and SVC2 have different design values. The circuit diagram of the 380-V, 50-Hz harmonic-treated TCR based SVC is shown in Figure 6.

If the delta-connected static compensator is designed such that it can balance the active current components of the load phase currents when one of them is zero and the other two phase currents are carrying their rated currents with unity power factor, this will imply according to (13) that the balanced active line currents drawn from the AC supply are of 142.67A (peak value). Assuming that the phase of zero current is Phase C and applying (17)-(19) for calculating the compensating susceptances result in:  $B_{S1AB} = 0$ ,  $B_{S1BC} = 0.265\bar{U}$ , and  $B_{S1CA} = -0.265\bar{U}$ . According to these calculated susceptances, SVC1 should be designed such that its capacitive and inductive reactive current ratings are equal. This implies that the factor  $k_R$  employed in (38) should be of a value of 2. Using (47) after substituting for  $V_{AC}$  by 537V and for  $B_S$  by  $0.265\bar{U}$  results in a reactive current rating of 142.67A (peak value). Note that 537V stands for the peak value of an rms value of 380V. Consequently, the TCR reactor of SVC1 should carry a reactive current of 283.333A (peak value). Since the peak value of the AC voltage across the TCR is 537V, the following design values are computed:  $L_T=6\text{mH}$ ,  $L_1=2.916\text{mH}$ ,  $L_2=1.75\text{mH}$ ,  $L_3=1.25\text{mH}$ ,  $L_S=3.07\text{mH}$ ,  $C_S=3300\mu\text{F}$ ,  $C_1=387\mu\text{F}$ ,  $C_2=231\mu\text{F}$ , and  $C_3=165\mu\text{F}$ . Note that  $L_T$  is calculated by dividing 537 by  $283.333\omega$  and other design quantities are calculated using (27)-(30) and (40)-(43). Self-resistances of reactors are chosen such that for each reactor the resistance to inductance ratio is about  $10\Omega$  per Henry. The thyristor used for TCR design is of the type T627121574DN. It has continuous voltage and current ratings of 2200V and 300A, respectively. This SVC is excited by the instantaneous line voltage  $v_L$  which is of peak to peak value of 1075V. Its phase is chosen to be zero for simplicity. The currents  $i_S$ ,  $i_F$ , and  $i_T$  stand for the instantaneous currents of SVC1, filtering circuit, and the

TCR, respectively.  $v_T$  represents the instantaneous voltage across the TCR. SVC1 current controller and thyristor driving circuit are represented by electronic parts saved in certain locations on PSpice libraries.

The controller of the harmonic-treated TCR current is driven by the analogue voltage  $k_2 B_S$  shown in Figure 4. The controller of Figure 4 represents a general controlling scheme of the harmonic-treated TCR. The basic controlling signal in the 380-V, 50-Hz harmonic-treated TCR is  $k_4 B_S$  which is represented by a DC voltage supply varying in the range of -10V to +10V. The controlling circuit of SVC1 is shown in Figure 7. This circuit is thoroughly emulating the controlling scheme depicted in Figure 4. Since  $k_R$  for SVC1 is 2, the constant  $A_1$  and  $A_2$  are calculated to be 0.5 and 0.25, respectively. The electronic part F(ALPHA) is saved in a separate library on PSpice. The constant  $k_4$  is calculated as follows:  $k_4 = 10V / (142.67A / 537V) = 37.64V\Omega$ .

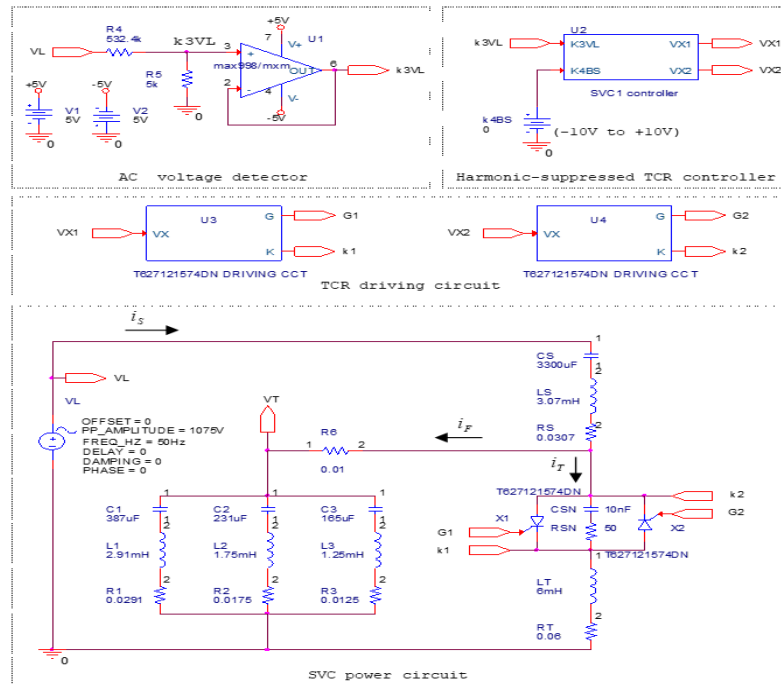
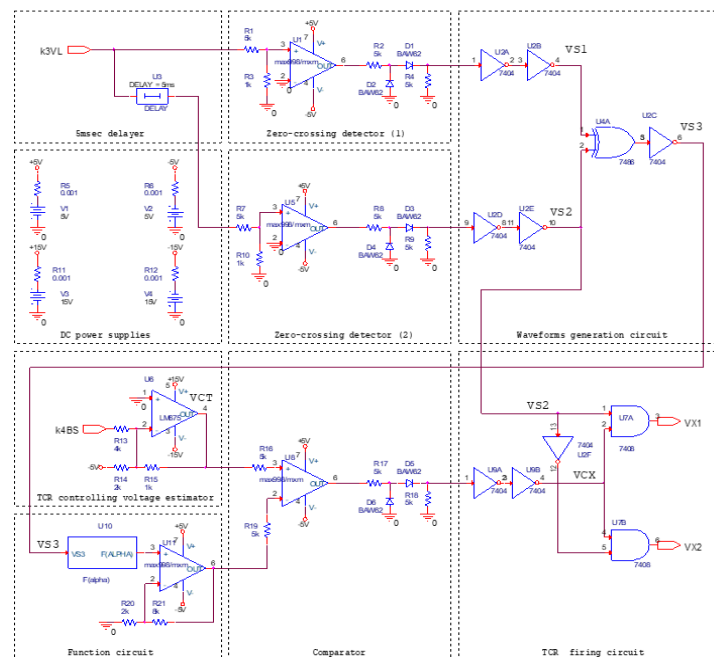


Figure 6. The circuit diagram of the 380-V, 50-Hz harmonic-treated TCR based SVC (type SVC1)



The driving circuit of the thyristor T627121574DN used in the design of SVC1 is shown in Figure 8. The circuit supplies the sufficient gate current to the thyristor during the active pulse across the gate and cathode. In addition, it offers through its opto-coupler the suitable electrical isolation between the power circuit and the low voltage electronic circuits.

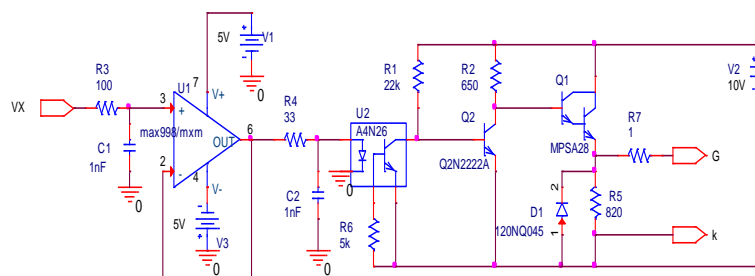


Figure 8. The driving circuit of the thyristor T627121574DN

The electronic part that stands for F(ALPHA) in the SVC1 controlling circuit is generated on PSpice using the electronic circuit shown in Figure 9. In this figure, a signal analogous to the mathematical behavior of in (24) is produced. The input to this circuit is the rectangular waveform  $V_{S3}$  which is generated through the X-NOR operation on  $V_{S1}$  and  $V_{S2}$ . Many electronic operations are used in the simulation of  $F(\alpha)$ . A ramp signal is produced due the exertion of  $V_{S3}$  on the ramp generator. Many electronic processes are made on the ramp signal such that a positive half-cycle of a sinusoidal signal running at double frequency of the AC source is produced. Comparing  $V_{CT}$  with  $5F(\alpha)$  makes the TCR current fundamental respond linearly to the reactive current demand, thus the overall response of SVC1 is linearized due to such a comparison. Linearizing the reactive current response of the harmonic-treated TCR based SVC to the reactive current demand is considered as another modification beside the harmonic treatment made on the traditional TCR. These two modifications promote such kinds of SVCs to be continuously and linearly controlled harmonic-free compensating susceptances. Figure 10 shows the waveforms of the analogue simulation of  $F(\alpha)$ .

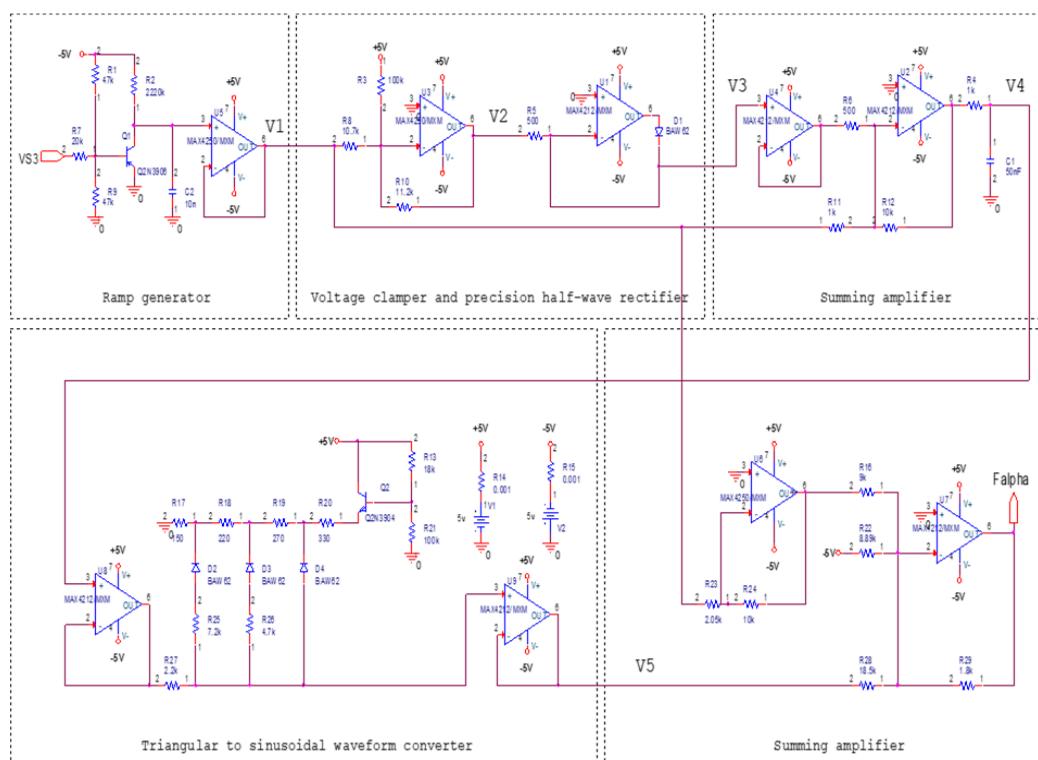


Figure 9. The analogue simulation of  $F(\alpha)$

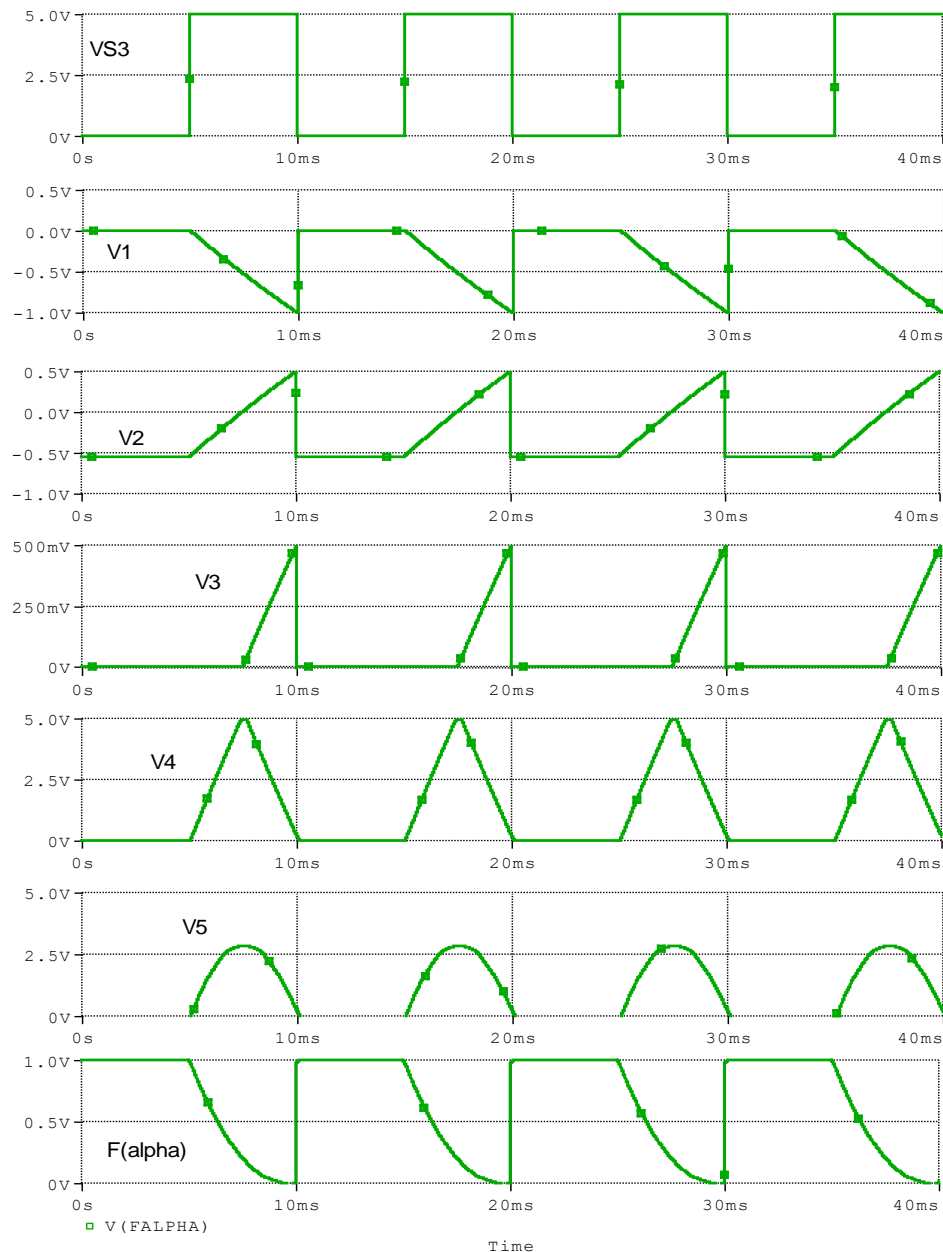


Figure 10. Waveforms indicating the production processes of  $F(\alpha)$

### 2.3. Circuit design of the 220-V, 50-Hz harmonic-treated TCR based SVC

This harmonic-treated TCR based SVC is the building block of the star-connected static compensator which is built to compensate for load reactive current components in addition to the reactive current components released by the first static compensator. It is classified as SVC2 type. The inductive and capacitive ratings for this SVC can be determined by considering the severe unbalance case associating the open circuit occurring on one phase of a three-phase load and the other two phases remain carrying the rated current with 0.8 lagging power factor. The maximum active current component of the line current of the first static compensator is  $0.8(214+214)/3=114\text{A}$  (peak value). The reactive current component associating this current is  $99\text{A}$  (peak value). The number 99 corresponds to  $114 \times \sin(\pi/3)$ . The reactive component of the first static compensator line current is either capacitive or inductive. Since the connected phases are carrying rated currents with 0.8 lagging power factor, an additional capacitive reactive of about  $128\text{A}$  (peak value) should be added to the reactive current of  $99\text{A}$  released by the first static compensator. The maximum expected capacitive current demanded from SVC2 is  $227\text{A}$  (peak value), while the maximum expected inductive current is about  $123\text{A}$  (peak value) which corresponds to  $142.67 \times \sin(\pi/3)$ . The TCR should satisfy a reactive current rating equal to the sum of the capacitive and inductive current ratings, i, e it should

be capable of carrying a maximum reactive current of 350A (peak value). Since the voltage applied across the TCR of SVC2 is a phase voltage of an rms value of 220V, the inductance of the TCR reactor ( $L_T$ ) is calculated to be about 2.83mH. The rating factor  $k_R$  of SVC2 is calculated according to its reactive currents rating to be  $350/227=1.542$ . Using Equations (40)-(43) results in the following design quantities:  $L_I=1.06\text{mH}$ ,  $L_2=0.63\text{mH}$ ,  $L_3=0.45\text{mH}$ , and  $L_S=1.13\text{mH}$ . The inductance value of  $L_S$  corresponds to a  $C_S$  value of more than  $8000\mu\text{F}$ . An inductance of about 2mH for  $L_S$  is a better choice for the harmonic-suppressing circuit, since it results in better reduction of harmonics and more acceptable value for  $C_S$ . Using the above design values for reactors and substituting them in (27)-(30) yield the following values for capacitors:  $C_S=5000\mu\text{F}$ ,  $C_I=1060\mu\text{F}$ ,  $C_2=645\mu\text{F}$ , and  $C_3=460\mu\text{F}$ . Self-resistances of reactors are chosen in the same manner adopted in SVC1. The circuit diagram of SVC2 is shown in Figure 11. The thyristor used in the circuit design of 220-V, 50-Hz harmonic-suppressed TCR based SVC is T627121574DN. The basic controlling signal in this SVC is  $k_5B_S$  which is varying in the range of -5.4V to +10V. SVC2 is excited by the phase voltage  $V_P$  which is of a peak to peak value of 622V. Since the maximum capacitive current of SVC2 corresponds to  $k_5B_S$  of 10V, then  $k_5$  is calculated as  $10\text{V}/(227\text{A}/311\text{V})=13.7\text{V}\Omega$ . 311V corresponds to the amplitude of 220V rms voltage. Since  $k_R$  for SVC2 is of a value of about 1.542, the constants  $A_1$  and  $A_2$  are calculated to be 0.649 and 0.325, respectively.

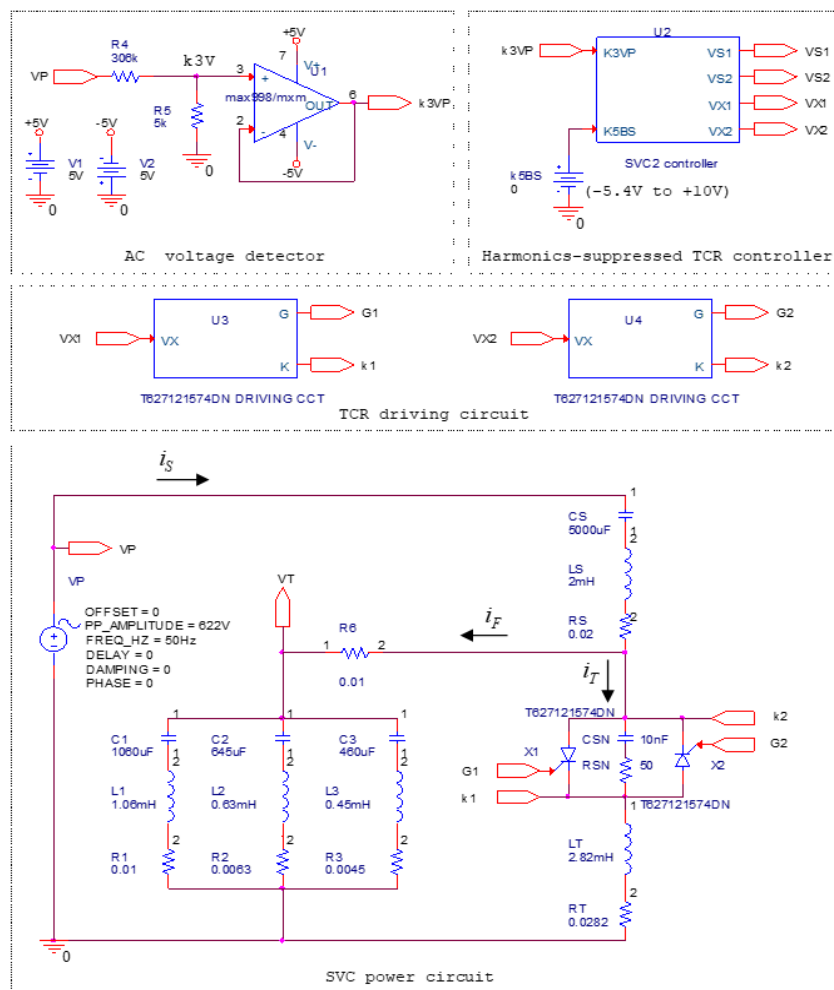


Figure 11. The circuit of the 220-V, 50-Hz harmonic-treated TCR based SVC (type SVC2)

#### 2.4. Circuit design of the proposed load current balancing system for grounded loads

Figure 12 shows the circuit diagram of a complete load current balancing system for grounded loads using two configurations of harmonic-treated TCR based SVCs. The first configuration represents a static compensator built of three SVCs type SVC1 connected in delta-form, while the second configuration is a static compensator built of three SVCs type SVC1 connected in star-form. The functions of the two

compensators are already discussed. Each SVC has its individual controller and driving circuit. The controllers are also discussed and the two driving circuits of the TCR thyristors are merged into one electronic part and saved in PSpice libraries. The circuit diagram includes a circuit called AC signals detection circuit which extracts low voltage analogue signals proportional to the phase and line voltages of the AC power system. The computation circuit in this circuit diagram is represented by a single electronic part.

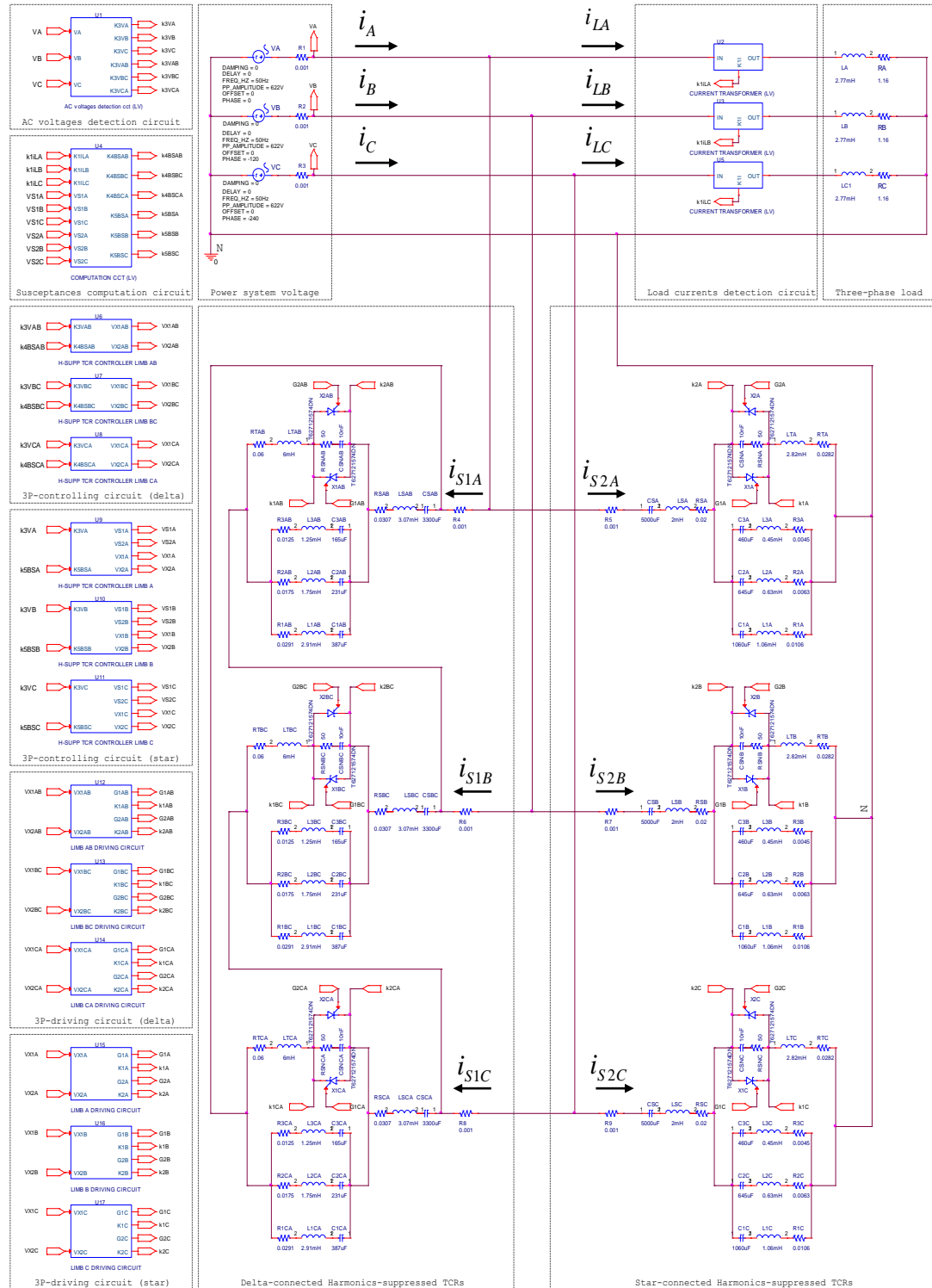


Figure 12. Circuit diagram of load current balancing system for grounded loads in 380-V, 50-Hz power system network using harmonic-treated TCR based SVCs

The AC voltage's detection circuit is shown in Figure 13. The phase voltages are detected through potential dividers which are buffered through three voltage followers. The buffers outputs are processed through difference amplifiers for demining the  $k_3v_{AB}$ ,  $k_3v_{BC}$ , and  $k_3v_{CA}$  which are necessary for the controllers of the delta-connected SVCs. According to this circuit,  $k_3$  is calculated to be 0.00892. The buffer outputs  $k_3v_A$ ,  $k_3v_B$ , and  $k_3v_C$  are necessary for the star-connected SVCs controllers and the computation circuit.

The current transformer used in this load current balancing system is shown in Figure 14. Its primary to secondary turn ratio is 1:100. The value of the resistance  $R_I$  is chosen such that the maximum amplitude of the analogue voltage  $k_I i$  is about 14.14V when the load line current is 214A (peak value). Accordingly,  $k_I$  is calculated to be  $0.066\Omega$ .

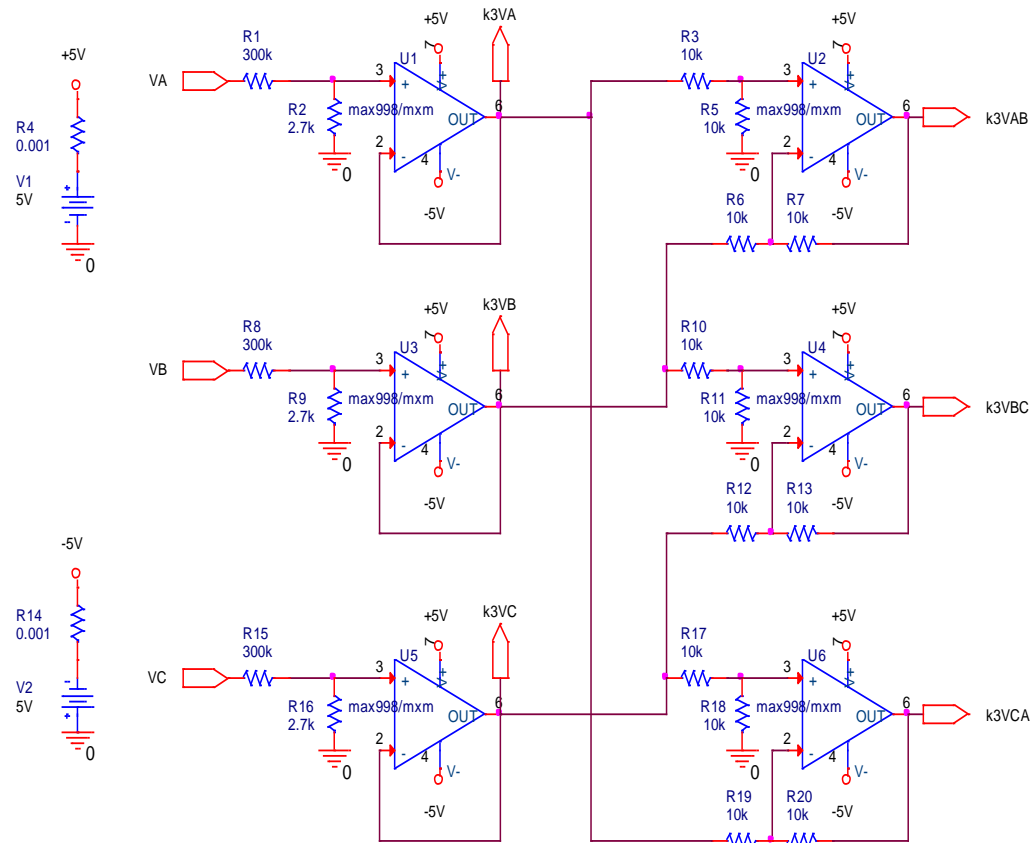
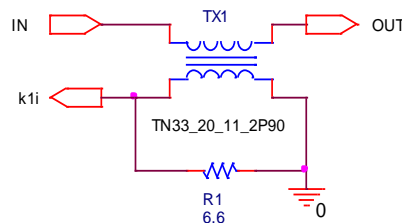


Figure 13. AC voltages detection circuit for load current balancing system using harmonic-treated TCR based SVCs



Primary to secondary turn ratio=1:100

Figure 14. Current transformer for 380-V, 50-Hz load current balancing system

The computation circuit is used to determine the compensating susceptances required for load current balancing. Its circuit diagram is shown in Figure 15. Firstly, the current signals are sampled at the



positive peaks of their corresponding phase voltages to obtain their active components. The current signals are also sampled at the negative slope zero-crossing points of their corresponding phase voltages to obtain the negative values of their reactive components. The delta-connected compensator susceptances are computed using (17)-(19), while the star-connected compensator susceptances are computed by using (20)-(22). The difference and summing amplifiers perform the computation process for all compensating susceptances.

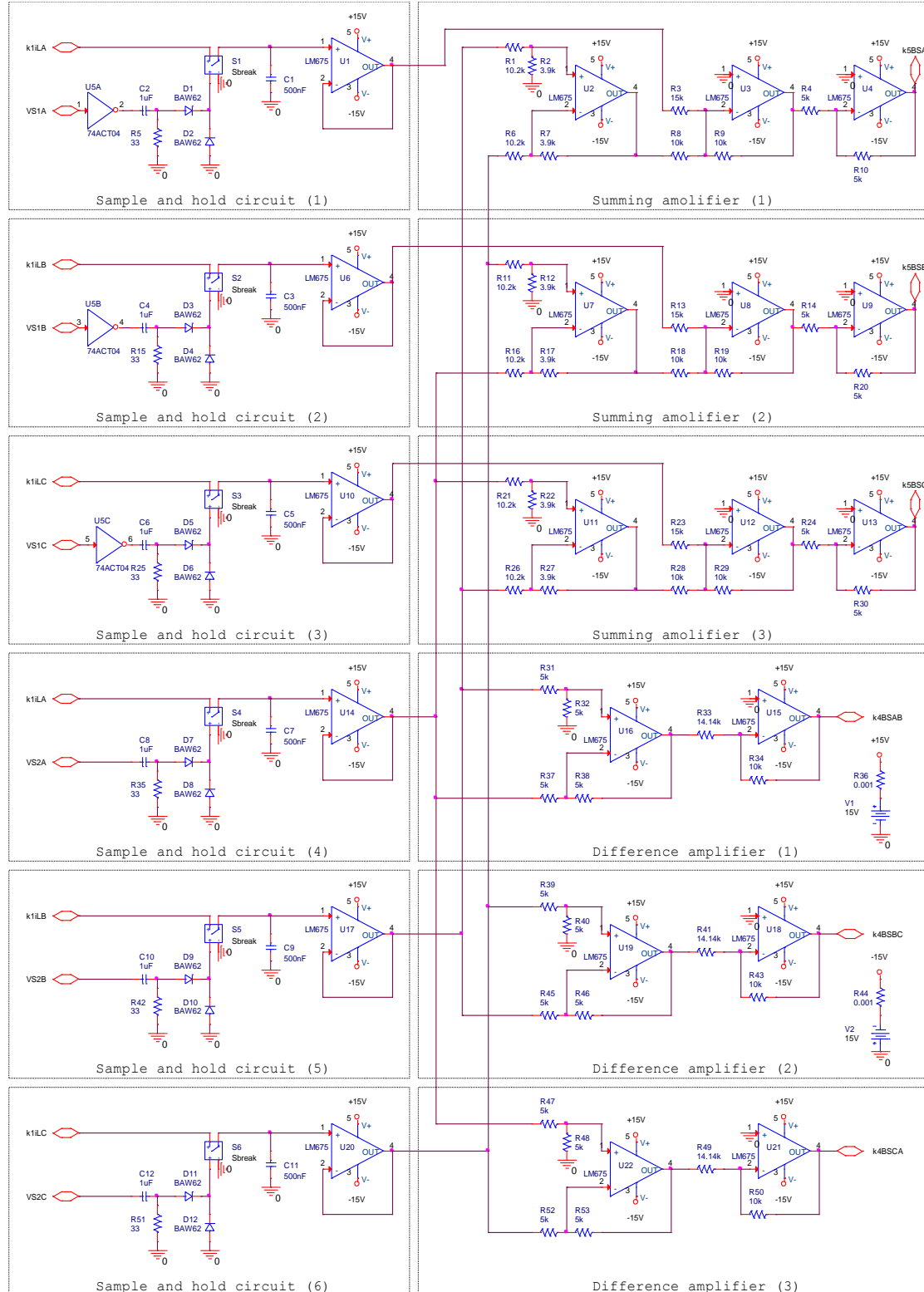


Figure 15. The computation circuit of load current balancing system using harmonic-treated TCR



### 3. RESULTS AND DISCUSSION

The circuits of Figures 6, 11, 12 were tested on PSpice to show the performance of the proposed compensating susceptances and load current balancing system.

#### 3.1. Performance results of the 380-V, 50-Hz harmonic-treated TCR based SVC

The 380-V, 50-Hz harmonic-treated TCR based SVC is classified as type SVC1. The circuit diagram of SVC1 is shown in Figure 6. This circuit was tested on PSpice for the investigation of harmonic contents, control continuity and linearity. The parameters measured through PSpice tests were the SVC current  $i_s$ , the TCR current  $i_T$ , the AC voltage  $v_L$ , the TCR voltage  $v_T$ , the SVC current frequency spectrum  $F(S)$ , and the TCR current frequency spectrum  $F(T)$ . The AC voltage  $v_L$  was of amplitude of 537V (peak value) and zero phase angle. The basic controlling signal of the compensator is  $k_4B_S$  which is represented by a separate DC source. Figure 16 shows SVC1 response to zero reactive current demand which corresponded to  $k_4B_S=0$ . It is obvious that SVC1 fundamental current is almost zero and  $F(S)$  is free from any sort of current harmonics. Figure 17 shows SVC1 response to an inductive current demand of 36A (peak value), which corresponded to  $k_4B_S$  of -2.5V. Figure 18 reflects SVC1 performance during its response to an inductive reactive current demand of 72A (peak value), which corresponded to  $k_4B_S$  of -5V. Figure 19 shows the performance of SVC1 during its response to an inductive reactive current demand of 108A (peak value) which corresponded to  $k_4B_S$  of -7.5V.

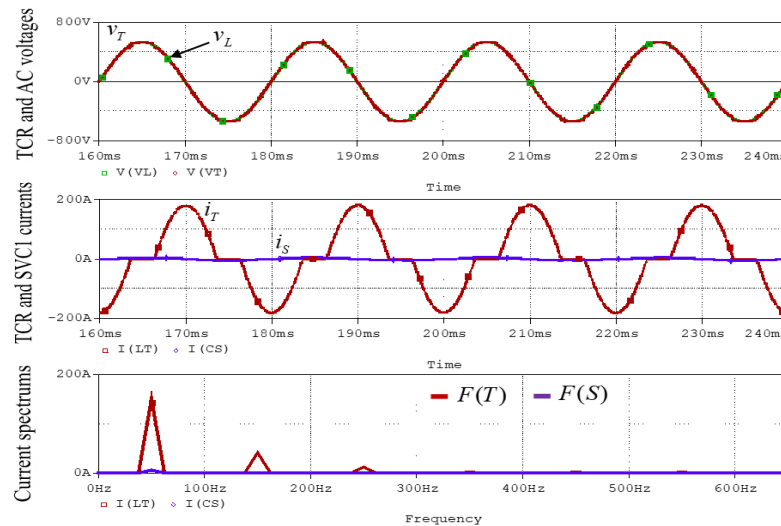


Figure 16. SVC1 response to zero reactive current demand

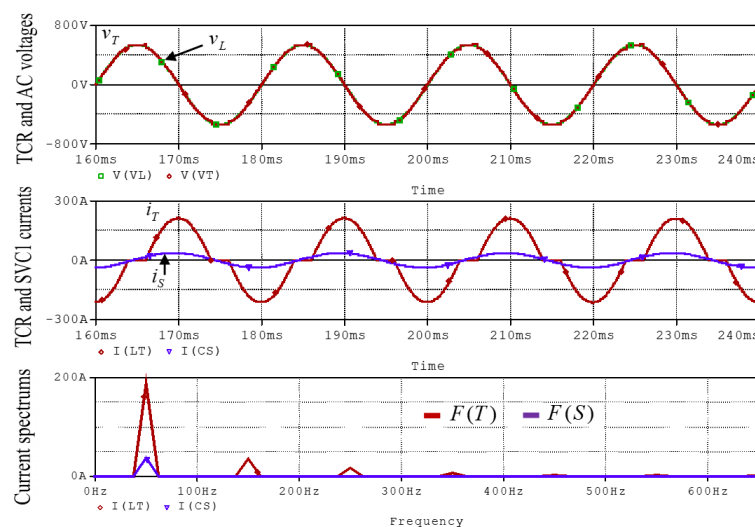


Figure 17. SVC1 response to an inductive current demand of 36A (peak value)

Figure 20 shows the performance of SVC1 during its response to an inductive current demand of 144A (peak value), which corresponded to  $k_4 B_S$  of -10V. This inductive reactive current demand corresponds to the compensator maximum inductive current rating. The TCR was operating at zero firing angle at this test. In all these tests, the compensator current was purely inductive. Even though the frequency spectrum of the TCR current  $F(T)$  exhibits significant odd current harmonics, SVC1 current spectrum  $F(S)$  is free from noticeable current harmonics except the fundamental component. This is due to the harmonic cancellation efficiency of the filtering circuit and the harmonic suppression efficiency of the harmonic suppressing circuit. During zero reactive current demand, SVC1 current frequency spectrum exhibits a fundamental current component of a less than 3A (peak value). This amount of current is responsible for no load operating losses of this compensator.

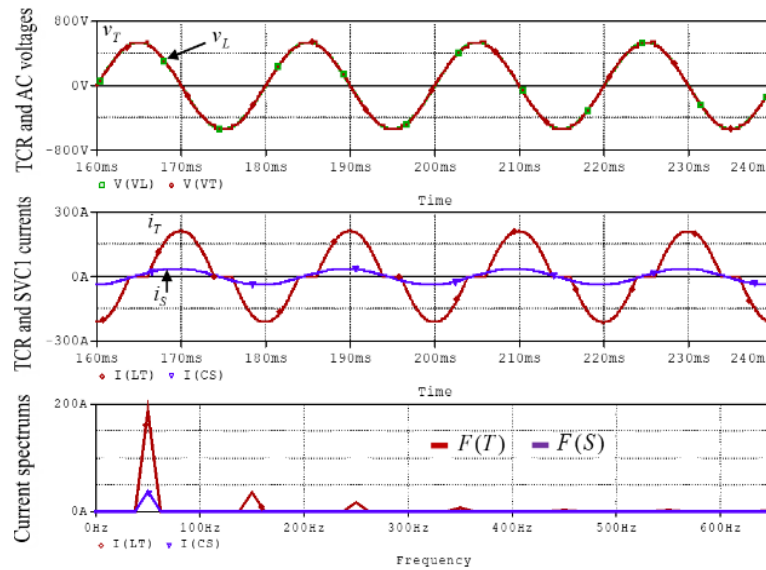


Figure 18. SVC1 response to an inductive current demand of 72A (peak value)

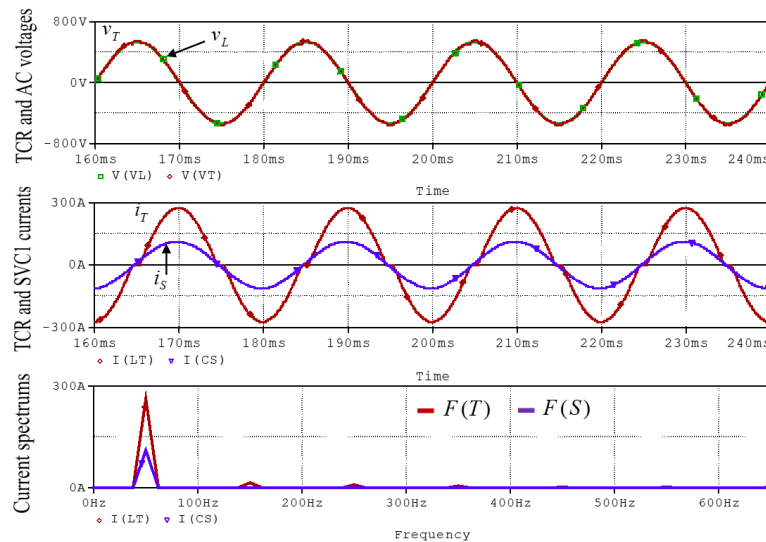


Figure 19. SVC1 response to an inductive current demand of 108A (peak value)

Here is the performance of SVC1 during capacitive mode of operation. Figure 21 shows the performance of SVC1 during its response to a capacitive reactive current demand of 36A (peak value), which corresponded to  $k_4 B_S$  of 2.5V. It is obvious that the compensator current waveform is purely capacitive. Figures 22-24 show the responses of SVC1 to capacitive reactive current demand of 72A, 108A, and 144A

(peak values) which, corresponded to  $k_d B_s$  of 5V, 7.5V, and 10V, respectively. The figures exhibit purely capacitive responses. During capacitive mode of operation, the frequency spectrum of SVC1 current indicates no noticeable current harmonics beside the fundamental component. In addition, the compensator current exhibits peaks at the positive slope zero crossing points of the AC voltage supplying the compensator. Consequently, SVC1 current is verified as purely capacitive and free from any sort of noticeable current components except the fundamental component. In Figure 24, the amount of current corresponds to SVC1 maximum capacitive current rating. In this test, the TCR was fully relaxed and filtering circuit was supplying the capacitive reactive current demand. The frequency spectrum of this test shows that the TCR current indicates no signs of harmonic association.

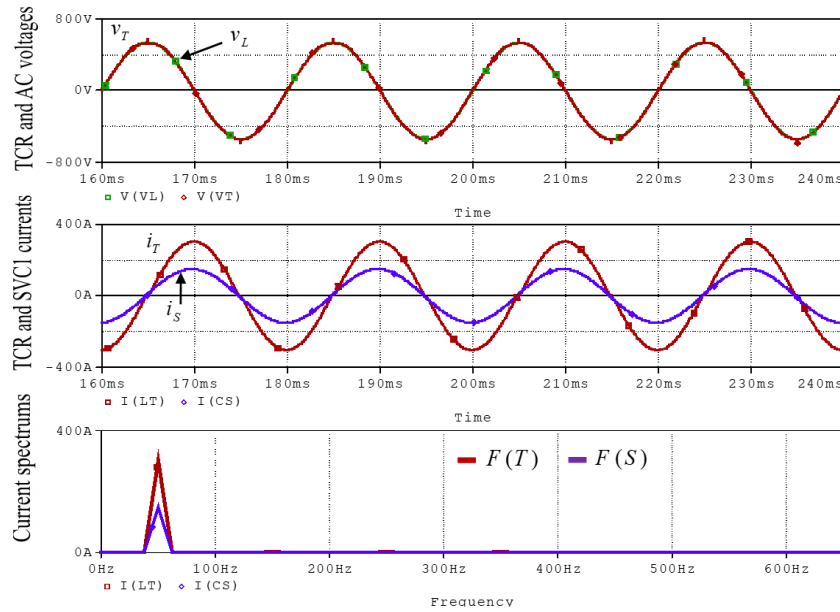


Figure 20. SVC1 response to an inductive current demand of 144A (peak value)

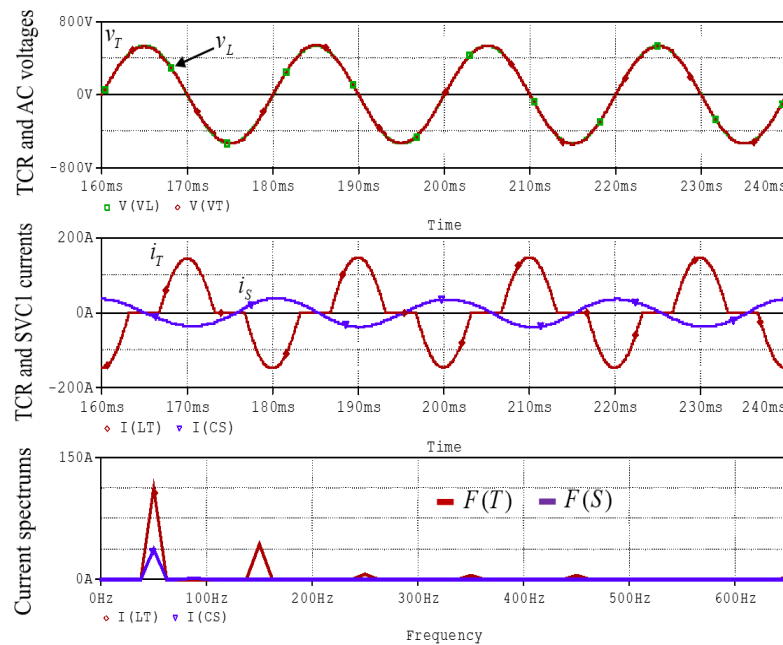


Figure 21. SVC1 response to a capacitive current demand of 36A (peak value)

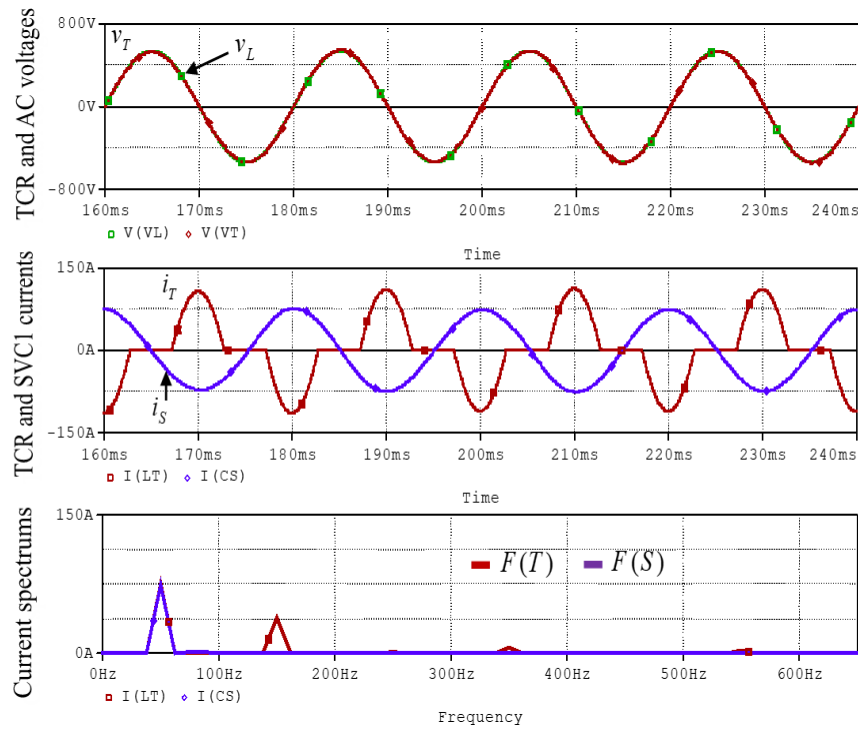


Figure 22. SVC1 response to a capacitive current demand of 72A (peak value)

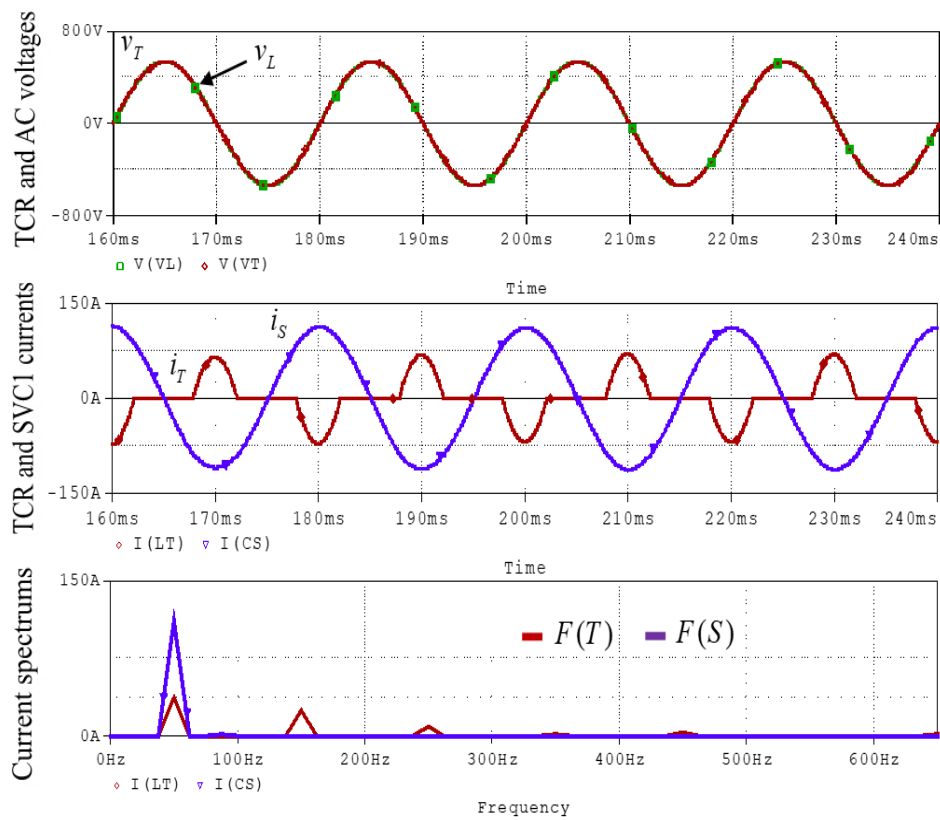


Figure 23. SVC1 response to a capacitive current demand of 108A (peak value)

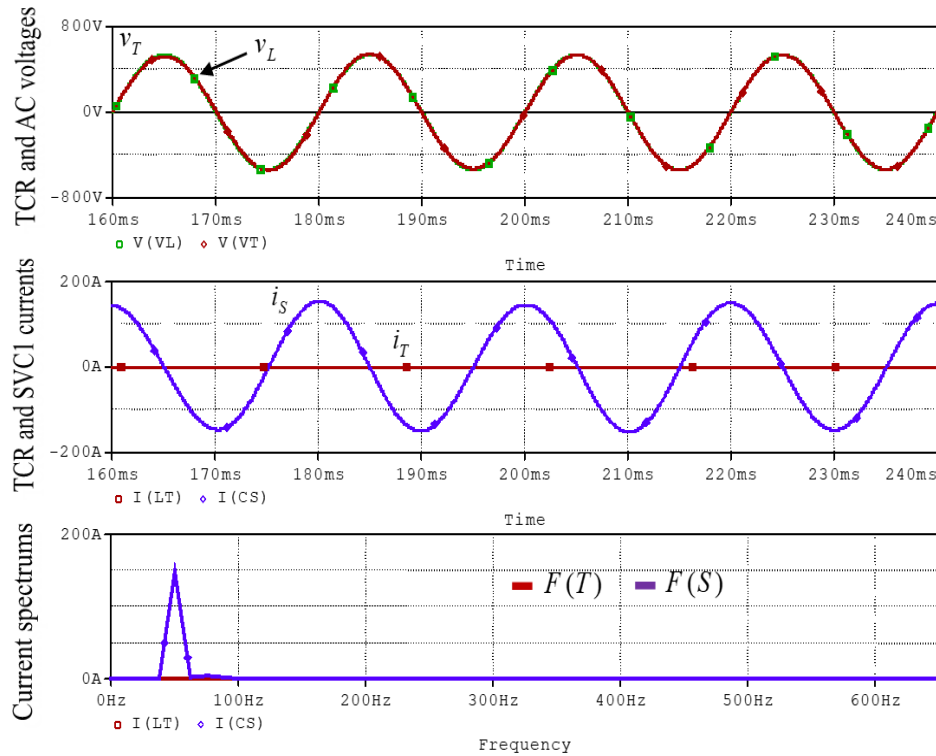


Figure 24. SVC1 response to a capacitive current demand of 144A (peak value)

According to the above tests, SVC1 is demonstrated as a harmonic-free pure reactive device which can be represented by a harmonic-free compensating susceptance. The nonexistence of any sort of current harmonics beside SVC1 reactive current fundamental reflects the effectiveness of the filtering technique adopted in the design of the harmonic-treated TCR. The linearity of the devised compensating susceptance is verified by the graph shown in Figure 25. This graph is obtained by plotting the actual values of SVC1 current against reactive current demand. The minus sign denotes inductive reactive current. The performance of this compensating susceptance during sudden change in reactive current demand from maximum capacitive to maximum inductive is shown in Figure 26.

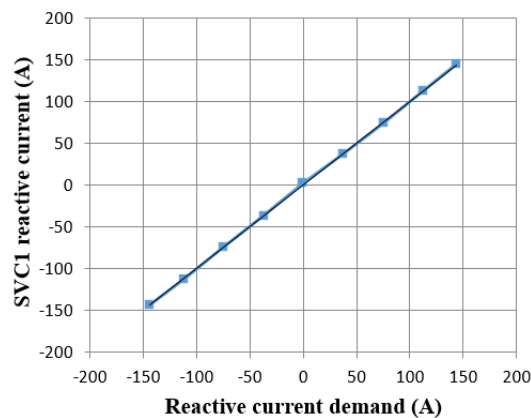


Figure 25. SVC1 actual reactive current against reactive current demand

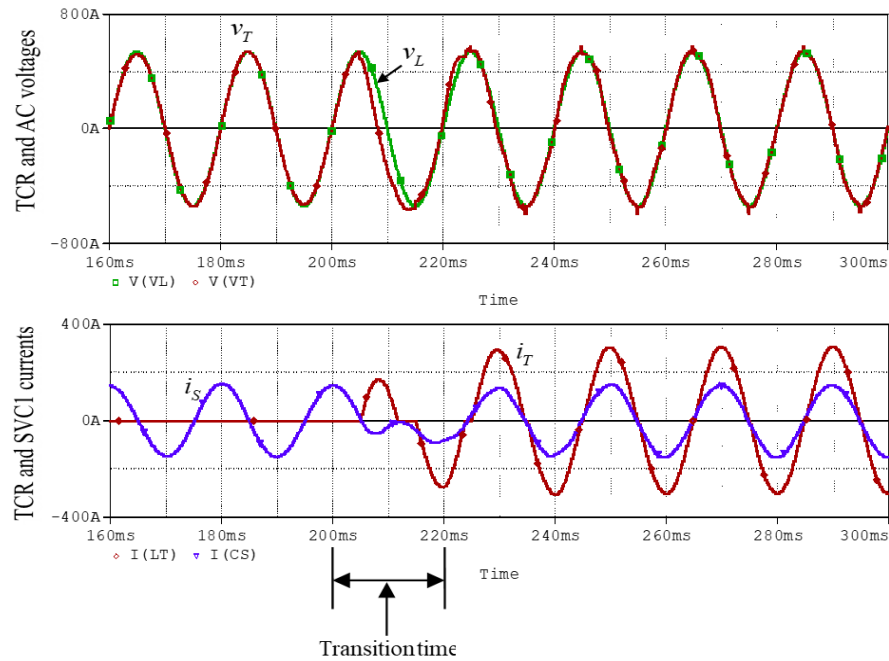


Figure 26. The treatment of SVC1 to sudden change in reactive current demand from maximum capacitive to maximum inductive. The change occurred at  $t=200\text{ms}$  and the transition period was 20ms

### 3.2. Performance results of the 220-V, 50-Hz harmonic-treated TCR based SVC

The 220-V, 50-Hz harmonic-treated TCR based SVC is classified as type SVC2. The circuit diagram of this SVC is shown in Figure 11. The AC voltage supplying SVC2 was the phase voltage  $v_P$  which was of amplitude of 311V (peak value) and zero phase angle. SVC2 is controlled by the analogue voltage  $k_5 B_s$ . A capacitive current of 227A (peak value) corresponds to  $k_5 B_s$  of 10V; while an inductive current of 123A (peak value) corresponds to  $k_5 B_s$  of -5.4V. A zero reactive current demand corresponds to  $k_5 B_s$  of zero value. SVC2 was tested on PSpice for the investigation of harmonic contents, control continuity and linearity. SVC2 shows similar performance compared to SVC1 in capacitive and inductive modes of operation, except different in reactive current ratings. SVC2 responses to reactive current demand variations in the range of 123A (peak value) inductive to 227A (peak value) capacitive are summarized as shown in Figure 27. The linearity of this susceptance is verified by the graph of this figure. This graph is obtained by plotting the actual current of SVC2 against reactive current demand. The minus sign in Figure 27 denotes inductive current. Finally, it has been demonstrated that the 220-V, 50-Hz harmonic-treated TCR based SVC (SVC2) can be represented by a continuously and linearly controlled harmonic-free compensating susceptance.

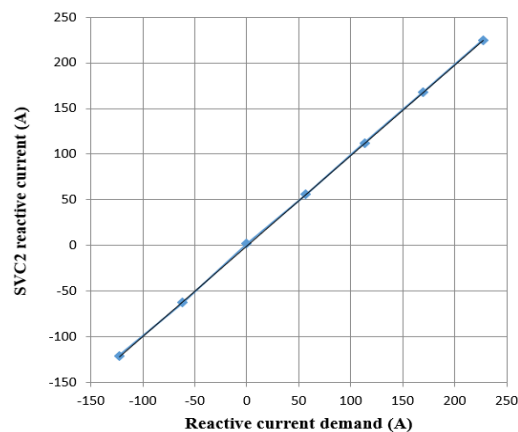


Figure 27. SVC2 reactive current against reactive current demand

### 3.3. Performance results of the proposed load current balancing system

This load balancing system is shown in Figure 12. The system was tested on PSpice at different loading conditions. The basic parameters measured were the AC source currents  $i_A$ ,  $i_B$ , and  $i_C$ ; the load currents  $i_{LA}$ ,  $i_{LB}$ , and  $i_{LC}$ ; the first compensator currents  $i_{S1A}$ ,  $i_{S1B}$ , and  $i_{S1C}$ ; the second compensator currents  $i_{S2A}$ ,  $i_{S2B}$ , and  $i_{S2C}$ . The AC source was a 100-kVA, 11 kV/380 V, 50-Hz power transformer having a rated current of 214 A (peak value). Figure 28 shows the compensator performance during balanced rated resistive load. It is obvious that the load current balancing system was relaxed through this test since both its compensators were carrying almost zero currents.

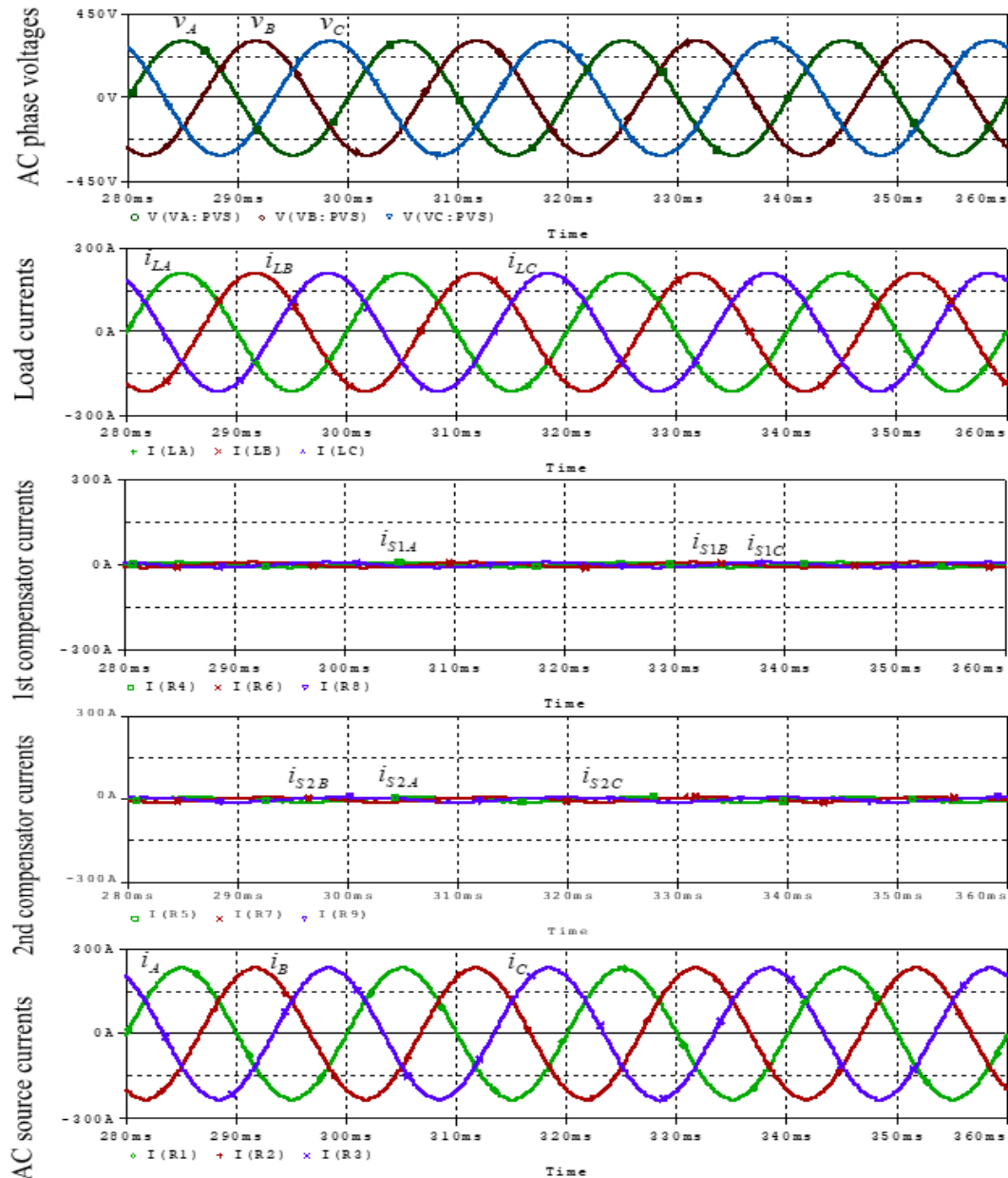


Figure 28. The proposed load current balancing system was relaxed during balanced resistive load

Figure 29 shows the treatment of the load current balancing system to a balanced three-phase load carrying the power transformer rated current at a lagging power factor of 0.707. The treatment had resulted in balanced resistive load drawn from the power transformer. During this load, the first compensator of the load current balancing system was fully relaxed. The figure shows big reduction in the AC source currents.



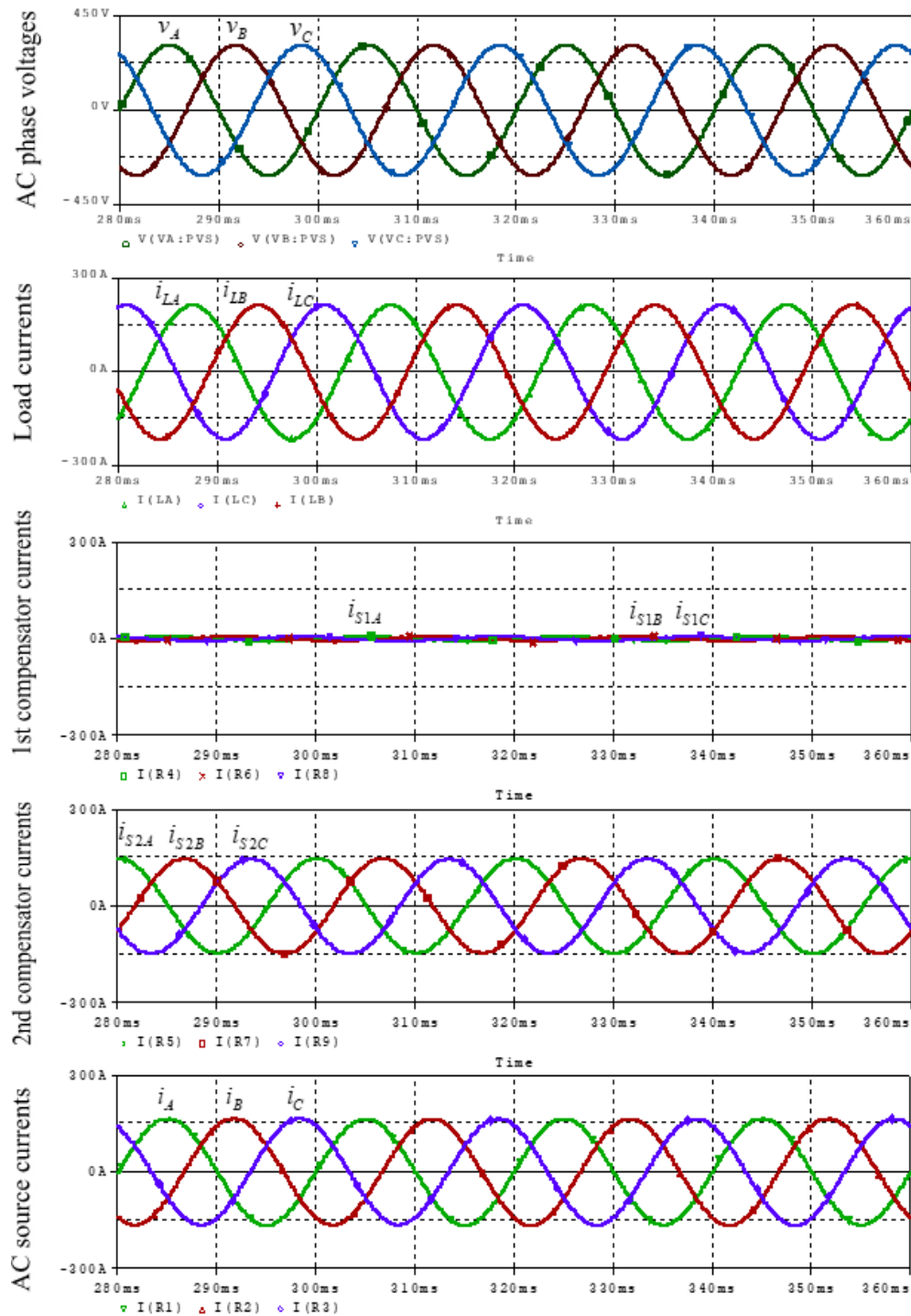


Figure 29. The proposed load current balancing system during its treatment to a balanced rated load at 0.707 lagging power factor

The system can correct to unity the power factor of the load phase currents as long as the load reactive current components are within the reactive current capability of the second compensator. If the reactive current contents required to be compensated are exceeding the second compensator capability, then the expected action will be power factor improvement of the load phase currents. Figure 30 shows the performance of the load current balancing system during a load unbalance resulted from disconnecting one phase of a balanced rated load at a lagging power factor of 0.8. Even though, the load unbalance was severe, it had been recovered with balanced pure real currents drawn from the AC source (power transformer).



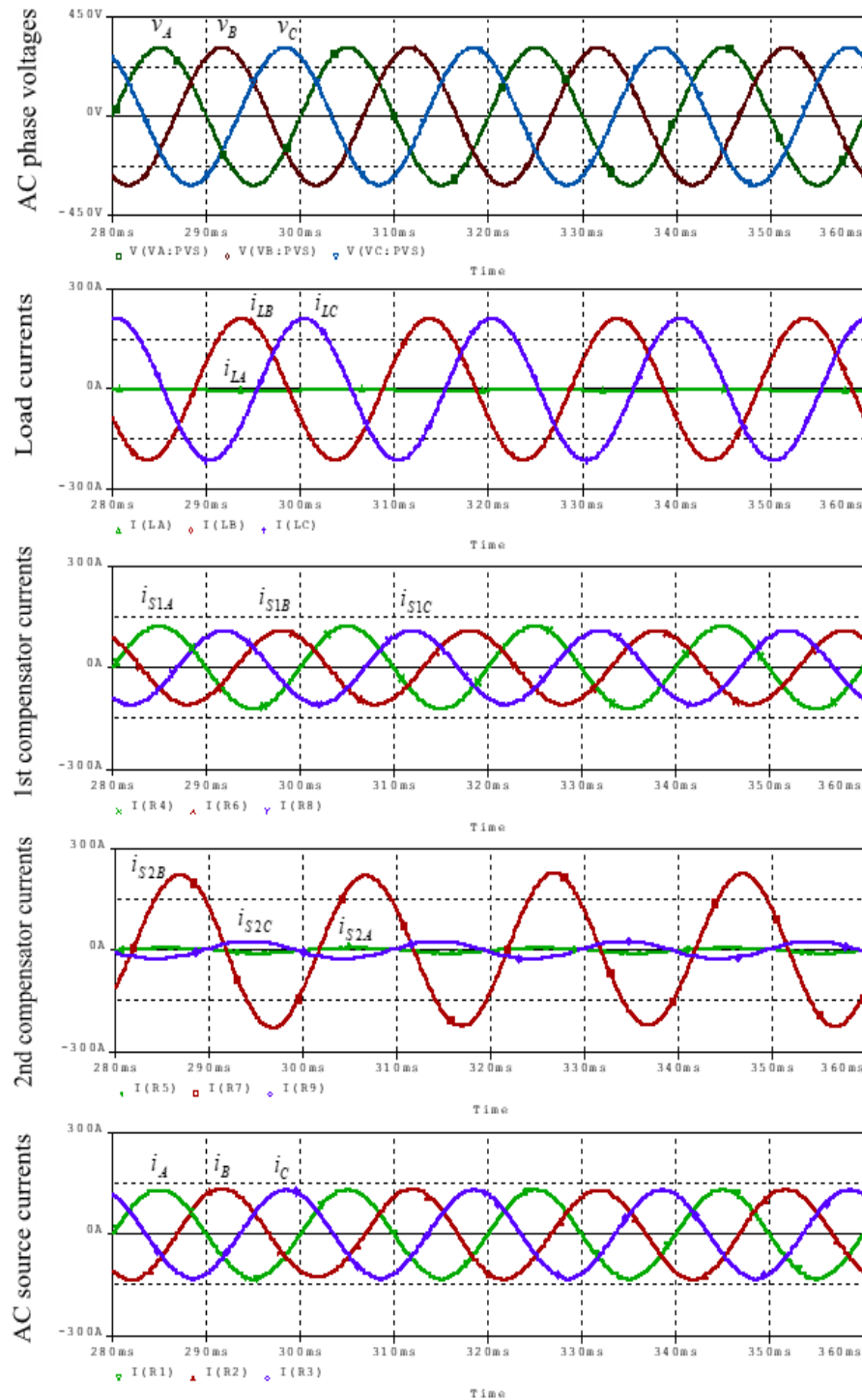


Figure 30. Performance of the proposed load current balancing system during the disconnection of one phase of a balanced rated load at 0.8 lagging power factor

Figure 31 shows the treatment of a load unbalance resulted from the disconnection of two phases of a rated three-phase load at 0.8 lagging power factor. The above load unbalance is actually severe, but the load current balancing system had easily involved it with the production of balanced active AC source phase currents. Figure 32 shows the treatment of a significant unbalance in phase and magnitude of a three-phase load having phase currents exceeding the power transformer current rating. The load balancing system had brought the AC source currents below their rated values. The compensation mechanism of the load unbalance depicted in Figures 32 is clarified by the phasor diagram shown in Figure 33.

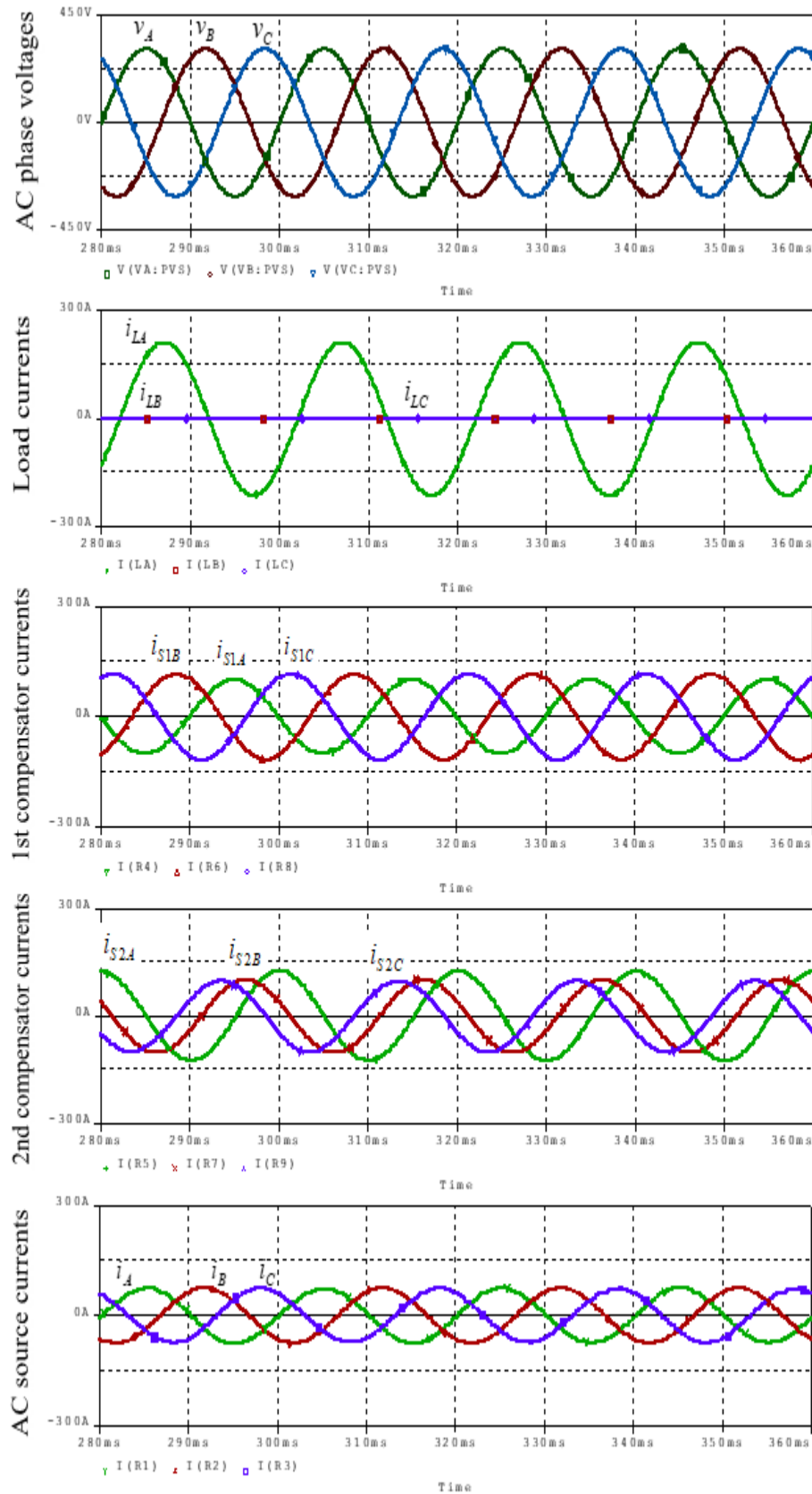


Figure 31. Performance of the proposed load current balancing system during the disconnection of two phases of a three-phase load and leaving the third carrying a rated current at 0.8 lagging power factor

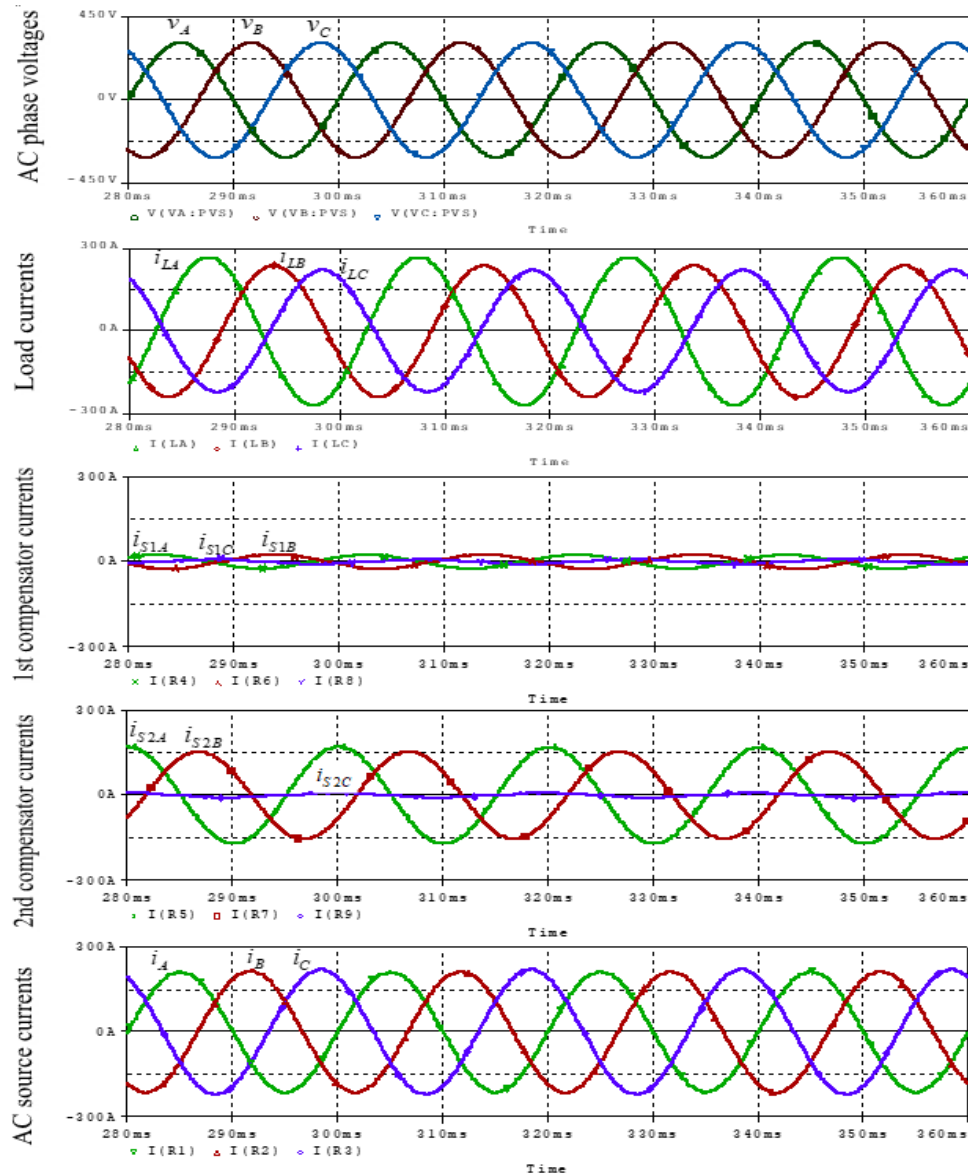


Figure 32. Performance of the load current balancing system during its treatment to a load unbalance in which all phase currents were exceeding the power transformer rating

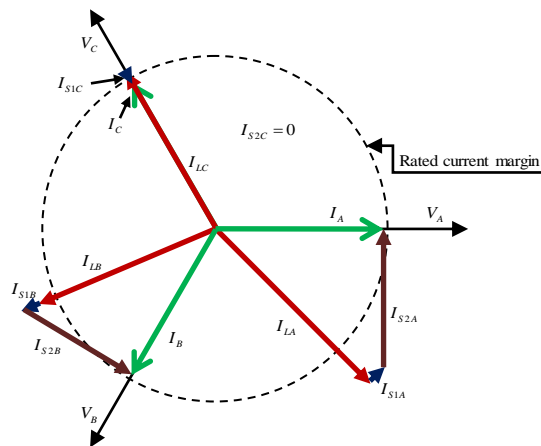


Figure 33. A phasor diagram showing the balancing mechanism of the load unbalance treated in Figure 32

#### 4. CONCLUSION

The harmonic-treated TCR based SVC is devised from the traditional TCR, which is characterized by the injection of wide spectrum of odd current harmonics. Equipping the traditional TCR with efficient harmonic-suppressing and filtering circuits beside the devised controlling scheme makes it respond linearly to reactive current demand (capacitive and inductive) without noticeable harmonic association. The filtering efficiency of the devised SVC is invulnerable to the adjacent harmonic sources in the power system network where the SVC is installed. The 3<sup>rd</sup>, 5<sup>th</sup>, and 7<sup>th</sup> current harmonics are completely cancelled in the SVC current, while the 9<sup>th</sup> odd harmonic and forth are minimized to at least one tenth their magnitudes in the TCR current. The harmonic-treated TCR based SVC represents a reliable replacement of the FC-TCR based SVC equipped with high power harmonic filters, thus using harmonic-treated TCR based SVC achieves energy and cost savings. In addition, this devised SVC is capable of satisfying reactive current demand during sudden change from maximum capacitive to maximum inductive with a transition time less than 20msec. The devised continuously and linearly controlled harmonic-free compensating susceptances are employed in the design of a transformerless load current balancing system for a 100-kVA power transformer in a 380-V, 50-Hz distribution network. The devised compensating susceptances and the designed load current balancing are characterized by controlling linearity and compensation quality superior to those proposed by previous works. The proposed load current balancing system had showed excellent treatment to different unbalance conditions.




#### REFERENCES

- [1] J. E. R. Alves, L. A. S. Pilotto and E. H. Watanabe, "Thyristor-Controlled Reactors Nonlinear and Linear Dynamic Analytical Models," *IEEE Transactions on Power Delivery*, vol. 23, no. 1, pp. 338-346, 2008, doi: 10.1109/TPWRD.2007.911131.
- [2] B. Singh, P. Jayaprakash, T. R. Somayajulu and D. P. Kothari, "Reduced Rating VSC With a Zig-Zag Transformer for Current Compensation in a Three-Phase Four-Wire Distribution System," *IEEE Transactions on Power Delivery*, vol. 24, no. 1, pp. 249-259, 2009, doi: 10.1109/TPWRD.2008.2005398.
- [3] A. Luo, Z. Shuai, W. Zhu and Z. J. Shen, "Combined System for Harmonic Suppression and Reactive Power Compensation," *IEEE Transactions on Industrial Electronics*, vol. 56, no. 2, pp. 418-428, 2009, doi: 10.1109/TIE.2008.2008357.
- [4] Y. Xu, L. M. Tolbert, J. D. Kuek, and D. T. Rzy, "Voltage and current unbalance compensation using a static VAR compensator," *IET Power Electronics*, vol. 3, no. 6, pp. 977-988, 2010, doi: 10.1049/iet-pel.2008.0094.
- [5] A. Hamadi, S. Rahmani and K. Al-Haddad, "A Hybrid Passive Filter Configuration for VAR Control and Harmonic Compensation," *IEEE Transactions on Industrial Electronics*, vol. 57, no. 7, pp. 2419-2434, 2010, doi: 10.1109/TIE.2009.2035460.
- [6] B. Singhy and P. Venkateswarlu, "A Simplified Control Algorithm for Three-Phase, Four-Wire Unified Power Quality Conditioner," *Journal Power Electronics*, vol. 10, no. 1, pp. 91-96, 2010, doi: 10.6113/JPE.2010.10.1.091.
- [7] J. Wu, H. Jou, H. Hsiao and S. Xiao, "A New Hybrid Power Conditioner for Suppressing Harmonics and Neutral-Line Current in Three-Phase Four-Wire Distribution Power Systems," *IEEE Transactions on Power Delivery*, vol. 29, no. 4, pp. 1525-1532, 2014, doi: 10.1109/TPWRD.2014.2322615.
- [8] W.N. Chang and K.D. Yeh, "Real-time load balancing and power factor correction of three-phase, four-wire unbalanced systems with DSTATCOM," *Journal Marine Science Technology*, vol. 22, no. 5, pp. 598-605, 2014, doi:10.6119/JMST-013-0926-1.
- [9] L. S. Czarnecki and P. M. Haley, "Unbalanced Power in Four-Wire Systems and Its Reactive Compensation," *IEEE Transactions on Power Delivery*, vol. 30, no. 1, pp. 53-63, 2015, doi: 10.1109/TPWRD.2014.2314599.
- [10] A. Hintz, U. R. Prasanna and K. Rajashekara, "Comparative Study of the Three-Phase Grid-Connected Inverter Sharing Unbalanced Three-Phase and/or Single-Phase systems," *IEEE Transactions on Industry Applications*, vol. 52, no. 6, pp. 5156-5164, 2016, doi: 10.1109/TIA.2016.2593680.
- [11] X. Zhao, C. Zhang, X. Chai, J. Zhang, F. Liu and Z. Zhang, "Balance control of grid currents for UPQC under unbalanced loads based on matching-ratio compensation algorithm," *Journal of Modern Power Systems and Clean Energy*, vol. 6, no. 6, pp. 1319-1331, 2018, doi: 10.1007/s40565-018-0383-7.
- [12] Y. Hoon and M. A. M. Radzi, "PLL-Less Three-Phase Four-Wire SAPF with STF-dq0 Technique for Harmonics Mitigation under Distorted Supply Voltage and Unbalanced Load Conditions," *Energies*, vol. 11, no. 8, pp. 1-27, 2018, doi: 10.3390/en11082143.
- [13] C. Cai, P. An, Y. Guo, and F. Meng, "Three-Phase Four-Wire Inverter Topology with Neutral Point Voltage Stable Module for Unbalanced Load Inhibition," *Journal of Power Electronics*, vol. 18, no. 5, pp. 1315-1324, 2018, doi: 10.6113/JPE.2018.18.5.1315.
- [14] L. S. Czarnecki, "CPC – Based Reactive Balancing of Linear Loads in Four-Wire Supply Systems with Nonsinusoidal Voltage," *Przegląd Elektrotechniczny*, vol. 95, no. 4, pp. 1-8, 2019, doi:10.15199/48.2019.04.01.
- [15] H. Yoon, D. Yoon, D. Choi, and Y. Cho, "Three-Phase Current Balancing Strategy with Distributed Static Series Compensators," *Journal of Power Electronics*, vol. 19, no. 3, pp. 803-814, 2019, doi: 10.6113/JPE.2019.19.3.803.
- [16] G. Bao and S. Ke, "Load Transfer Device for Solving a Three-Phase Unbalance Problem under a Low-Voltage Distribution Network," *Energies*, vol. 12, no. 15, pp. 1-18, 2019, doi: 10.3390/en12152842.
- [17] Z. Soljan, G. Holdyński, and M. Zajkowski, "Balancing reactive compensation at three-phase four-wire systems with a sinusoidal and asymmetrical voltage source," *Bulletin of the Polish Academy of Sciences*, vol. 68, no. 1, pp. 71-79, 2020, doi: 10.24425/bpasts.2020.131831.
- [18] Z. Zhang, "Design of alternating current voltage-regulating circuit based on thyristor: Comparison of single phase and three phase," *Measurement and Control*, vol. 53, no. 5-6, pp. 884-891, 2020, doi: 10.1177/0020294020909123.
- [19] A. A. Goudah, D. Schramm, M. El-Habrouk, A. A. Farag, and Y. G. Dessouky, "Smart Electric Grids Three-Phase Automatic Load Balancing Applications Using Genetic Algorithms," *Journal of Renewable Energy and Sustainable Development (RES D)*, vol. 6, no. 1, 2020, doi: 10.21622/RES D.2020.06.1.018.
- [20] C. Li, Z. Xia, F. Li, X. Chen, H. Li, Z. Liu, and G. Wang, "Unbalanced current analysis of three-phase AC-DC converter with




- power factor correction function based on integrated transformer,” *IET Power Electronics*, vol. 13, no. 12, pp. 2461-2468, 2020, doi: 10.1049/iet-pel.2019.1415.
- [21] R. M. Mira, P. A. Blasco, J. M. Diez, R. Montoya, and M. J. Reig, “Unbalanced and Reactive Currents Compensation in Three-Phase Four-Wire Sinusoidal Power Systems,” *Applied Sciences*, vol. 10, no. 5, pp. 1-23, 2020, doi:10.3390/app10051764.
- [22] P. A. Blasco, R. Montoya-Mira, J. M. Diez, and R. Montoya, “An Alternate Representation of the Vector of Apparent Power and Unbalanced Power in Three-Phase Electrical Systems,” *Applied Sciences*, vol. 10, no. 11, pp. 1-16, 2020, doi: 10.3390/app10113756.
- [23] K. Ma, L. Fang and W. Kong, “Review of distribution network phase unbalance: Scale, causes, consequences, solutions, and future research directions,” *CSEE Journal of Power and Energy Systems*, vol. 6, no. 3, pp. 479-488, 2020, doi: 10.17775/CSEEJPES.2019.03280.
- [24] M. N. Ansari, and R. K. Singh, “Application of D-STATCOM for Harmonic Reduction using Power Balance Theory,” *Turkish Journal Computer and Mathematics Education*, vol. 12 no. 6, pp. 2496-2503, 2021, doi: 10.17762/turcomat.v12i6.5694.
- [25] R. A. Otto, T. H. Putman and L. Gyugyi, “Principles and Applications of Static, Thyristor-Controlled Shunt Compensators,” *IEEE Transactions on Power Apparatus and Systems*, vol. PAS-97, no. 5, pp. 1935-1945, 1978, doi: 10.1109/TPAS.1978.354690.
- [26] L. T. G. Lima, A. Semlyen and M. R. Iravani, “Harmonic domain periodic steady state modeling of power electronics apparatus: SVC and TCSC,” *IEEE Transactions on Power Delivery*, vol. 18, no. 3, pp. 960-967, 2003, doi: 10.1109/TPWRD.2003.813805.
- [27] S. S. A. Dangeti, C. K. P. Sekharamanthy, V. K. Bayanti, B. A. R. Ch, K. R. Murthy, and A. Tirupathi, “A cascaded converter using hybrid cells and H-bridge structure,” *Bulletin of Electrical Engineering and Informatics*, vol. 10, no. 6, pp. 2972-2979, 2021, doi: 10.11591/eei.v10i6.2783.
- [28] K. M. Abdulhassan and O. Y. K. Al-Atbee, “Improved modified a multi-level inverter with a minimum total harmonic distortion,” *Bulletin of Electrical Engineering and Informatics*, vol. 11, no. 2, pp. 672-680, 2022, doi: 10.11591/eei.v11i2.3466.
- [29] A. K. Mishra, S. R. Das, P. K. Ray, R. K. Mallick, A. Mohanty and D. K. Mishra, “PSO-GWO Optimized Fractional Order PID Based Hybrid Shunt Active Power Filter for Power Quality Improvements,” *IEEE Access*, vol. 8, pp. 74497-74512, 2020, doi: 10.1109/ACCESS.2020.2988611.
- [30] K. V. G. Rao and M. Kiran Kumar, “The harmonic reduction techniques in shunt active power filter when integrated with non-conventional energy sources,” *Indonesian Journal of Electrical Engineering and Computer Science*, vol. 25, no. 3, pp. 1236-1245, 2022, doi: 10.11591/ijeecs.v25.i3.pp1236-1245.
- [31] A. Ram, P. R. Sharma, and R. K. Ahuja, “Performance evaluation of different configurations of system with DSTATCOM using proposed **Icos $\phi$**  technique,” *Indonesian Journal of Electrical Engineering and Computer Science*, vol. 25, no. 1, pp. 1-13, 2022, doi: 10.11591/ijeecs.v25.i1.pp1-13.

## BIOGRAPHIES OF AUTHORS



**Abdulkareem Mokif Obais**    was born in Iraq in 1960. He received his BSc. and M.Sc. degrees in Electrical Engineering from the University of Baghdad, Baghdad, Iraq, in 1982 and 1987, respectively. He received his PhD degree in Electrical Engineering from Universiti Tenaga Nasional, Kajang, Malaysia in 2013. He is interested in electronic circuit's design and power electronics. He had supervised and examined a number of postgraduate students. He had published many papers in Iraqi academic and international Journals. Dr. Obais was promoted to Professor at University of Babylon in April 2008. He can be contacted at email: eng.abdul.kareem@uobabylon.edu.iq.



**Ali Abdulkareem Mukheef**    was born in Iraq in 1995. He received his BSc. and M.Sc. degrees from University of Babylon, Iraq in 2016 and 2020, respectively. He is one of the Academic Staff of Almustaqbal University College, Babylon, Iraq. Presently, he is a PhD student at University of Babylon, Babylon, Iraq. He can be contacted at email: ali.abdulkreem@mustaqbal-college.edu.iq.